

Stephen F. Austin State University

SFA ScholarWorks

Electronic Theses and Dissertations

5-2021

A Multifunctional Solution Composed Of TMPyP, 1,5-DHN, And Fe(III) Ions That Produces Reactive Oxygen Species (ROS) In Aerobic, Anaerobic, And H₂O₂ Environments

Aqeeb Ali

Stephen F Austin State University, aqeeb999@gmail.com

Follow this and additional works at: <https://scholarworks.sfasu.edu/etds>

 Part of the [Organic Chemistry Commons](#)

[Tell us](#) how this article helped you.

Repository Citation

Ali, Aqeeb, "A Multifunctional Solution Composed Of TMPyP, 1,5-DHN, And Fe(III) Ions That Produces Reactive Oxygen Species (ROS) In Aerobic, Anaerobic, And H₂O₂ Environments" (2021). *Electronic Theses and Dissertations*. 374.

<https://scholarworks.sfasu.edu/etds/374>

This Thesis is brought to you for free and open access by SFA ScholarWorks. It has been accepted for inclusion in Electronic Theses and Dissertations by an authorized administrator of SFA ScholarWorks. For more information, please contact cdsscholarworks@sfasu.edu.

A Multifunctional Solution Composed Of TMPyP, 1,5-DHN, And Fe(III) Ions That Produces Reactive Oxygen Species (ROS) In Aerobic, Anaerobic, And H₂O₂ Environments

Creative Commons License



This work is licensed under a [Creative Commons Attribution-Noncommercial-No Derivative Works 4.0 License](https://creativecommons.org/licenses/by-nc-nd/4.0/).

A MULTIFUNCTIONAL SOLUTION COMPOSED OF TMPYP, 1,5-DHN, AND
Fe(III) IONS THAT PRODUCES REACTIVE OXYGEN SPECIES (ROS) IN
AEROBIC, ANAEROBIC, AND H₂O₂ ENVIRONMENTS

By

AQEER ALI, B.S. Chemistry

Presented to the Faculty of the Graduate School of
Stephen F. Austin State University
in Partial Fulfillment
Of the Requirements

For the Degree of
Masters of Natural Science in Chemistry

STEPHEN F. AUSTIN STATE UNIVERSITY

May, 2021

A MULTIFUNCTIONAL SOLUTION COMPOSED OF TMPYP, 1,5-DHN, AND
Fe(III) IONS THAT PRODUCES REACTIVE OXYGEN SPECIES (ROS) IN
AEROBIC, ANAEROBIC, AND H₂O₂ ENVIRONMENTS

By

AQEER ALI, B.S. Chemistry

APPROVED:

Dr. Matibur R. Zamadar, Thesis Director

Dr. Michele R. Harris, Committee Member

Dr. Xiaozhen Han, Committee Member

Dr. Robert Friedfeld, Committee Member

Pauline M. Sampson, Ph. D.,
Dean of Research and Graduate Studies

ABSTRACT

Photodynamic therapy (PDT) has become a widely popular therapeutic approach for treating various types of cancer over the past several decades. PDT utilizes a photosensitizer, visible light, and oxygen, to produce reactive oxygen species (ROS) which can be used to treat cancer and inhibit growth of bacteria. In this study, a multifunctional solution that is comprised of Fe(III) ions, cationic meso-tetra(N-methyl-4-pyridyl)porphine tetrachloride (TMPyP), and 1,5-dihydroxynaphthalene (1,5-DHN), was shown to produce reactive oxygen species (ROS) such as singlet oxygen ($^1\text{O}_2$) or hydroxyl radicals ($\dot{\text{O}}\text{H}$) in aerobic or anaerobic environments, respectively, and in both environments, 1,5-DHN was oxidized to Juglone or derivatives of Juglone. Moreover, this multifunctional solution was found to generate $\dot{\text{O}}\text{H}$ and Juglone in a hydrogen peroxide (H_2O_2) rich environment without the presence of visible light. This multifunctional solution has shown potential as a possible antibacterial agent and photosensitizer for PDT which possesses unique characteristics that can address many of the limitations and challenges in the field of PDT.

TABLE OF CONTENTS

ABSTRACT.....	i
LIST OF FIGURES	iv
LIST OF TABLES	vi
Chapter 1: Introduction.....	1
Chapter 2: Methods and Materials.....	6
Materials, Chemicals, and Stock Preparation	6
TMPyP, Fe(III) ions, and DHN Standard Mixture Preparation	7
Photooxidation of 1,5-dihydroxynaphthalene (DHN) by TMPyP in Aqueous Solution	7
Singlet Oxygen ($^1\text{O}_2$) Detection.....	8
Singlet Oxygen Quantum Yield (Φ_Δ) of TMPyP.....	8
Fluorescence Quantum Yield of TMPyP Using Crystal Violet as Known Standard	8
<i>In vitro</i> Effects of TMPyP with BL21 <i>E. coli</i>	9
Fluorescence Studies of TMPyP in combination with DHN and Fe(III) ions	10
The Optimization of Hydrogen Peroxide's Concentration by Oxidation of DHN	10
Effects of DHN Oxidation by Optimized Hydrogen Peroxide and Varying Fe(III) Ion Concentrations	11

MCF-7 Cell Culture	11
Treatment of MCF-7 Cells.....	12
Using MTS Assay for Determining Cell Viability	12
Chapter 3: Results and Discussion.....	13
Generation of Singlet Oxygen ($^1\text{O}_2$), Hydroxyl radical ($\dot{\text{O}}\text{H}$), and Juglone by the Multifunctional Treatment Composition Through Visible Light Irradiation and Aerobic Conditions	13
Generation of Hydroxyl radical ($\dot{\text{O}}\text{H}$) and Juglone by the Multifunctional solution in Anaerobic Condition with Visible Light Irradiation.....	24
Detoxification of H_2O_2 with Production of Hydroxyl Radicals and Juglone by Multifunctional Solution in the Absence of Visible Light	31
Fluorescence Study of the Multifunctional Treatment Composition and its Components.....	42
<i>In vitro</i> effects of the Multifunctional Treatment Composition, Under Visible Light Irradiation, on BL21 <i>E. coli</i> in Aerobic Conditions	44
<i>In vitro</i> effects of the Fenton-like reactions on BL21 <i>E. coli</i> in the Absence of Visible Light	48
<i>In vitro</i> effects of the Multifunctional Treatment Composition on MCF-7 Breast Cancer Cells	50
Chapter 4: Conclusion.....	52
References.....	54
Vita.....	60

LIST OF FIGURES

Figure 1: Structures for Fe(III)TMPyP, TMPyP, DHN, and Juglone.....	5
Figure 2: (a) The emissions plot for TMPyP (6.0×10^{-6} M) and SOSG in aqueous solution with a 532 nm laser for irradiation. (b) The SOSG peak at 525 nm after 60 minutes of irradiation by the 532 nm laser while recording the fluorescence spectra every 10 minutes.....	14
Figure 3: Photooxidation of DHN (1.2×10^{-4} M) by TMPyP (6.0×10^{-6} M) in aerobic aqueous solution.....	17
Figure 4: The calculated absorbance of DHN ($\ln(A_0)/(A)$) monitored at 301 nm as a function of irradiation time and Fe(III) ions concentration in aerobic aqueous solution .	19
Figure 5: The rate of change of DHN monitored at 301 nm as a function of irradiation time in D ₂ O, NaN ₃ , and H ₂ O	21
Figure 6: The rate of change for DHN peak at 301 nm when irradiated with 20 minutes of light in solutions with Fe(III)TMPyP, TMPyP and iron (II), and TMPyP and iron(III).....	23
Figure 7: The rate of change for DHN peak at 301 nm when irradiated with 20 minutes of light in solutions with Fe(III)TMPyP; TMPyP and iron (II); and TMPyP and iron (III) in anaerobic, aqueous solution.	27
Figure 8: The change in the absorbance peak (301 nm) of DHN in an anaerobic aqueous solution of just TMPyP and an anaerobic aqueous solution of TMPyP (6.0×10^{-6} M) and iron (III).....	28
Figure 9: The calculated absorbance of DHN ($\ln(A_0)/(A)$) monitored at 301 nm as a function of irradiation time in the presence of DHN and various amounts of Fe(III) concentrations in anaerobic aqueous solution.....	29
Figure 10: The rate of change for DHN peak at 301 nm when 1.0×10^{-6} M H ₂ O ₂ is added to the solution of Fe(III)TMPyP; TMPyP and iron (II); and TMPyP and iron (III) in aerobic, aqueous solution under dark conditions	34

Figure 11: (a) Optimization of H ₂ O ₂ concentration in the presence of 1 × 10 ⁻⁴ M iron (III) in aerobic, aqueous solution under dark conditions. (b) The UV-vis spectra of the recorded optimum H ₂ O ₂ concentration at 400 μM.....	35
Figure 12: (a) Optimization of iron (III) concentration in the presence of 400 μM iron (III) in aerobic, aqueous solution under dark conditions. (b) The UV-vis spectra of the recorded optimum iron (III) concentration at 25.0 μM.....	37
Figure 13: (a) Oxygen gas generation in an aqueous iron (III) (1.0 × 10 ⁻² M) and H ₂ O ₂ (1.0 × 10 ⁻² M).; (b) Oxygen gas measured by oxygen electrode in mV vs time (min).....	39
Figure 14: Dark precipitate in solution with Fe TMPyP (5.71 × 10 ⁻⁶ M), DHN (1.14 × 10 ⁻⁴ M) and H ₂ O ₂ (1.0 × 10 ⁻¹ M) after 18 hours	40
Figure 15: Emission spectra for TMPyP, iron (III), and DHN in aqueous solution.....	43
Figure 16: <i>E. coli</i> growth monitored after 48 hours, with (a) DHN (b) Juglone (c) TMPyP and Fe (III) (d) TMPyP and DHN (e) TMPyP, DHN, and iron (III) (f) TMPyP, Juglone, and iron(III)	47
Figure 17: <i>E. coli</i> growth, monitored after 48 hours, with (a) 1 × 10 ⁻⁴ M Fe (III) (b) 1 × 10 ⁻³ M Fe (III) (c) 400 μM H ₂ O ₂ (d) 1 × 10 ⁻⁴ M Fe (III) and 400 μM H ₂ O ₂ (e) 1 × 10 ⁻³ M Fe (III) and 400 μM H ₂ O ₂	49

LIST OF TABLES

Table 1: Summary of rate constants of DHN photo-oxidation by TMPyP as a function of [Fe (III) ions] in aerobic conditions.....	20
Table 2: Rates of photooxidation of DHN monitored at 301 nm as a function of irradiation time in the presence of Fe TMPyP, TMPyP and iron (II), and TMPYP and iron (III), respectively, in aerobic aqueous solution. k_{obs} is the rate constant (s^{-1}) of the DHN decay kinetics	24
Table 3: Summary of all the rate constants for the photooxidation of DHN by TMPyP as a function of [Fe (III) ions] in anaerobic conditions	30
Table 4: Survival of <i>Escherichia coli</i> in the presence of DHN, Juglone, Fe (III), and TMPyP with various combinations.....	44
Table 5: Percent survival of 10,000 MCF-7 cells in 10 minutes of light and dark condition where each trial's cell viability was measured immediately after treatment	51

CHAPTER 1

Introduction

As deaths due to cancer are increasing, researchers all around the world are working towards developing newer and more efficient therapeutic methods to treat cancer. Current cancer treatments include chemotherapy, radiation, and surgery which are limited because of their lack in selectivity of removing or killing tumors.¹ Newer treatment methods such as photodynamic therapy (PDT) can treat various types of cancers and is accepted as an effective and noninvasive treatment method.² PDT requires three components in order to be effective which are visible light, a photosensitizer, and dissolved oxygen. A photosensitizer can react with visible light and transfer energy to nearby dissolved oxygen (O_2) which will generate singlet oxygen (1O_2). Singlet oxygen is a type of reactive oxygen species (ROS) and is a key component in killing cancer cells.³⁻⁴ Although PDT shows promise in treating cancer, there are currently a few limitations to this therapeutic method. Firstly, the photosensitizer must be soluble in bodily tissue so that the photosensitizer can have sufficient localization to the tumor. Secondly, many large tumors that are in deeper tissues must be able to be penetrated by visible light or there will be no activation of the photosensitizer. Lastly, if a tumor that has become

hypoxic due to improper supply of blood, then PDT becomes ineffective since the therapy requires the presence of oxygen for producing singlet oxygen.⁵⁻⁷ Thus, to have effective therapeutic capability, there has been an increased interest in finding appropriate compounds that can address one or more of the limitations that PDT can experience.

A possible photosensitizer, that has become increasingly used in PDT to treat various types of cancers is a porphyrin called *meso*-tetra(4-*N*-methylpyridyl)porphine (TMPyP).⁸ TMPyP is a cationic porphyrin with four nitrogen atoms at the center of the molecule that can chelate various divalent metals. This molecule is also conjugated with double bonds which provides stability. A few characteristics that makes TMPyP a unique photosensitizer for PDT is that it is a water-soluble porphyrin and has the ability to be soluble in physiological liquids. Moreover, TMPyP requires no synthesis and can be acquired as a chemically pure and stable compound. In addition, TMPyP also has the capability of generating a high yield of singlet oxygen ($\Delta\Phi = 0.70$ in phosphate-buffered solution).⁹ Although this photosensitizer can address one of the limitations of PDT, it fails to produce ROSs in a hypoxic environment which is one of the major limitations of PDT. However, an advantage of TMPyP is that it has emissions in the red region and researchers can use this emission to study the localization of TMPyP. Villanueva and Patito, et al reported that TMPyP, at low concentrations, enters the cells via endocytosis and collects into lysosomes. Upon irradiation with visible light, ROS are produced which destroys the lysosome, distributing TMPyP into the nucleus and binding itself with DNA.¹⁰

Even with the excellent properties and characteristics of TMPyP, it is still unable to independently address the limitations of tumor hypoxia and the possibility of large tumors being impenetrable by visible light. To bypass the multiple limitations of PDT, another molecule or compound must be used in combination with TMPyP to create an effective treatment solution. Metals for example have been reported in the literature to be used as metal-based drugs for treating cancer. Cisplatin is a commonly known metal-based drug that has seen some success. However, these types of drugs face many challenges such as fatal side effects and poor water solubility and so more research in this area is needed to make further advancements.¹¹ In other research attempts, scientists have attempted to utilize unique, specific characteristics of cancer cells as a target for new therapeutic techniques. For instance, a specific characteristic of cancer cells is that they produce more hydrogen peroxide than normal cells.¹²⁻¹³ By taking advantage of the increased hydrogen peroxide produced from cancer cells, researchers can use iron-based methods to produce ROS via the Fenton reaction to kill those same cancer cells. For this reaction, Fe(II) ions can decompose hydrogen peroxide into hydroxyl radicals which are capable of damaging proteins, lipids, and DNA which leads to cell death.¹⁴⁻¹⁶ Although this is a feasible method, the Fenton reaction forms iron-containing sludge (Fe(OH)₃) as the reaction progresses which can lower the capability of producing hydroxyl radicals.¹⁷

For this project, an attempt is made to address several of PDT's limitations by studying a multifunctional system that is comprised of cationic meso-tetra(N-methyl-4-pyridyl)porphine tetrachloride (TMPyP), 1,5-dihydroxynaphthalene (1,5-DHN), and

Fe(III) ions which is not coordinated to the porphyrin ring (Figure 1). This treatment composition under visible light irradiation and aerobic environment produces, *in situ*, singlet oxygen, hydroxyl radical, and Juglone or its derivatives (non-toxic chemotherapeutic drugs). Furthermore, in an anaerobic environment, with visible light irradiation, the treatment composition is still able to produce hydroxyl radicals and Juglone or its derivative. Moreover, utilizing the increased hydrogen peroxide characteristic of cancer cells, the treatment composition undergoes a Fenton-like reaction which generates O_2 and hydroxyl radicals from hydrogen peroxide. This Fenton-like reaction is advantageous because no visible light is required for the production of hydroxyl radicals from hydrogen peroxide. This is a potential way to treat tumors that are deep in tissues and are unable to be penetrated by visible light. Moreover, the oxygen that is generated from the Fenton-like reactions can also be useful in situations of tumor hypoxia. With oxygen now being produced from the Fenton-like reactions, the photosensitizer can transfer its energy to oxygen and generate singlet oxygen under visible light conditions which is not possible without oxygen present. Lastly, using Fe(III) ions for the Fenton-like reaction does not produce an iron-containing sludge ($Fe(OH)_3$), so the production of hydroxyl radicals is not reduced. This treatment composition was also tested against *E. coli* in an aerobic environment with the presence and absence of visible light which showed some inhibition of growth. These results indicate that this multifunctional treatment solution can potentially treat bacteria and shows potential for treating cancer cells.

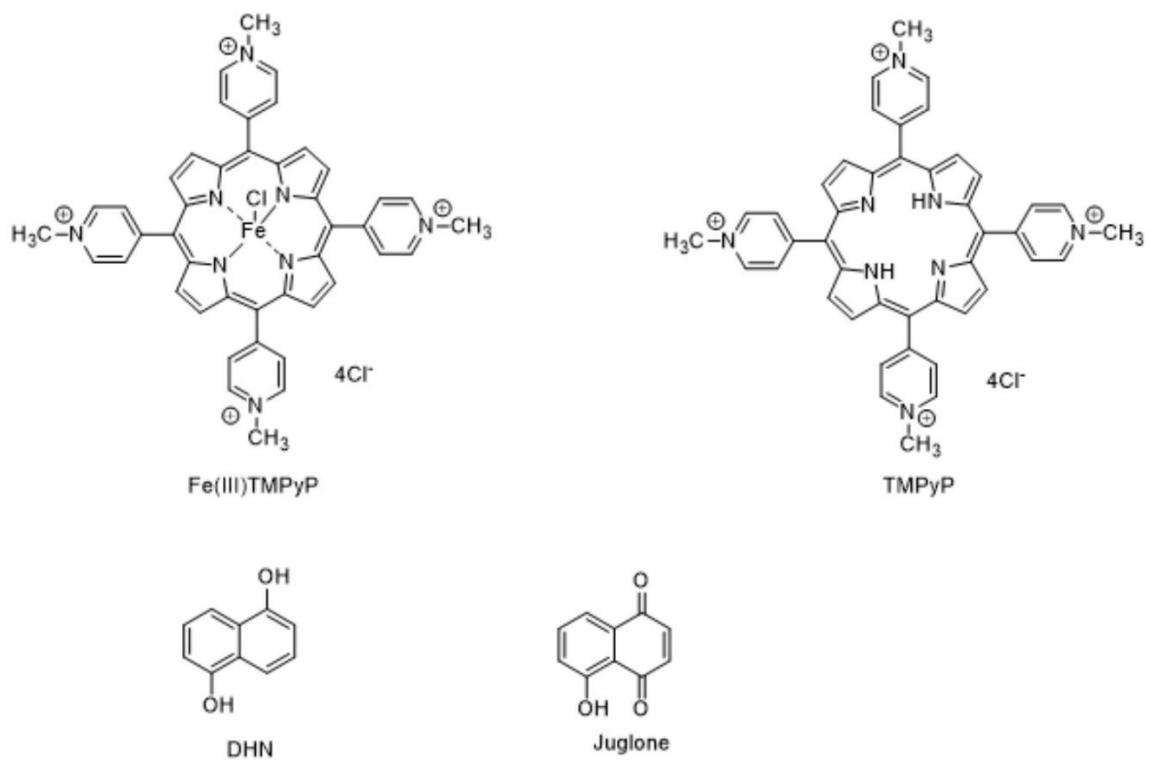


Figure 1. Structures for Fe(III)TMPyP, TMPyP, DHN, and Juglone.

CHAPTER 2

Methods and Materials

Materials, Chemicals, and Stock Preparation

Ultrapure H₂O (18.2 MΩ) was obtained from a U.S. Filter Corporation deionization system. Meso-tetra(N-methyl-4-pyridyl)porphine tetrachloride (TMPyP) and Fe(III)TMPyP were purchased from Frontier Scientific Inc., USA. 1,5-Dihydroxynaphthalene (DHN) and 5-hydroxy-1,4-naphthalenedione (Juglone) were received from Acros Organics. Iron (II) chloride and Iron (III) chloride were obtained from Flinn Scientific Inc., USA. Singlet oxygen sensor green (SOSG) was purchased from ThermoFisher Scientific Co., USA. 2-propanol was purchased from VWR analytical, USA, while p-nitrophenol, D₂O, NaN₃, and methylene blue were purchased from Sigma Aldrich, USA, these chemicals were used as received and no purification was needed. UV-vis spectra were recorded by using an Agilent 8453 single beam diode array spectrometer (Agilent Technologies, USA, model 8453). Fluorescence spectra were recorded by using a Perkin-Elmer LS-55, Fluorescence Spectrometer (Perkin-Elmer, USA) at room temperature. All the experiments requiring visible light irradiation were carried out on a Rayonet Chamber Reactor equipped with sixteen 5750Å lamps (The Southern New England Ultraviolet Co, USA, model RPR-100). A blue CW laser

(447 nm, 20 mW, 2.0 mm beam diameter), green CW laser (532 nm, 20 mW, 2.0 mm beam diameter), and CW laser (655 nm, 100 mW, Model: MRL-III-655-100mW 15060452) were purchased from Dragon Lasers CO, China.

TMPyP, Fe(III) ions, and DHN Standard Mixture Preparation

A standard solution of TMPyP (1.0×10^{-3} M), iron (III) chloride (1.0×10^{-2} M), and iron (II) chloride (1.0×10^{-2} M) were prepared in ultra-pure H₂O at room temperature under normal atmospheric conditions. The DHN (1.0×10^{-2} M) stock solution was prepared in a CH₃CN:H₂O (9:1, v/v) mixture solvents at room temperature. For a conventional experimental solution, 30 μ L of 1.0×10^{-2} M Fe(III) ions and 36 μ L of 1.0×10^{-2} M DHN was mixed in a cuvette with 3 mL of TMPyP at 6.00×10^{-6} M. Normally, a Quartz cuvette was used with a 1 cm path-length and volume of 3 mL for all measurements.

Photooxidation of 1,5-dihydroxynaphthalene (DHN) by TMPyP in Aqueous

Solution.

A 3 mL experimental solution containing DHN, at 1.2×10^{-4} M, and TMPyP, at 6.0×10^{-6} M, was prepared by mixing 36 μ L of 1×10^{-2} M of DHN and 18 μ L of 1×10^{-3} M of TMPyP with ultrapure water and normal atmospheric and room temperature conditions. The solution was irradiated with visible light in a Rayonet photoreactor for approximately twenty minutes at 28 °C. After every 2 minutes, the degradation of DHN was monitored by recording its decrease in absorption at 301 nm through UV-vis spectroscopy. The effect of metal ions on singlet oxygen generation was studied similarly

except with the addition of 30 μL amounts of M^{2+} ions (1×10^{-2} M) into a DHN/TMPyP aqueous solution.

Singlet Oxygen ($^1\text{O}_2$) Detection.

A 5 mM stock solution of SOSG was prepared by adding 33 μL of methanol to the 100 μg of SOSG sample. For each experiment, 6 μL of SOSG stock solution was placed into 3 mL of aqueous solution of TMPyP at 6.0×10^{-6} M. This sample solution was irradiated with a 532 nm CW laser and the fluorescence emission at 525 nm was recorded to monitor the production of singlet oxygen every 10 mins for a duration of 60 mins. (Fluorescence emission parameters are as follows: excitation at 504 nm, excitation slit 5 nm, emission slit 7 nm, speed 1000 nm/min, and a gain of medium.)

Singlet Oxygen Quantum Yield (Φ_{Δ}) of TMPyP.

The singlet oxygen quantum yield of TMPyP was determined using DHN at a concentration of 1.2×10^{-4} M as a singlet oxygen quencher and methylene blue (MB) as a reference standard. A 3 mL solution of TMPyP, at 6.0×10^{-6} M, and MB, at 1.0×10^{-5} M, were prepared. Each solution contained DHN at 1.2×10^{-4} M. Then, each solution was irradiated with a 655 nm CW laser and the UV-vis spectrum of the solution was recorded for 5 minutes at 1-minute intervals. The quantum yields were calculated with equation 1 by using known $\Phi_{\Delta(s)}$ of MB ($\Phi_{\Delta}=0.52$).¹⁸⁻¹⁹

Fluorescence Quantum Yield of TMPyP Using Crystal Violet as Known Standard

The experimental procedure for the fluorescence quantum yield of the TMPyP at a concentration of 6.0×10^{-6} M was followed using standard method described in

literature.^{18,20} Crystal violet (1.0×10^{-5} M) has a known fluorescence quantum yield (Φ_F) of 0.020 in water and was used as a standard.²¹

In vitro* Effects of TMPyP with BL21 *E. coli

To test the effects of singlet oxygen, BL21 *E. coli* cells were subjected to various combinations of aqueous solutions of TMPyP (6.0×10^{-6} M), DHN (1.2×10^{-4} M), Juglone (1.2×10^{-4} M), and iron (III) (1.0×10^{-4} M). The experimental group was subjected to the aqueous solutions while the control group was only contained sterile water. *E. coli* cell cultures were grown using reported literature protocol.²² In short, a colony of *E. coli* was allowed to grow overnight in Luria Broth (LB) in an incubator at 28°C and shaking at 250 rpm until the beginning of their exponential growth phase ($A_{600} = 0.2$). For each experiment, one milliliter aliquots of the *E. coli* solution were placed in microcentrifuge tubes and centrifuged. The resulting tube contained the *E. coli* pellet and the supernatant. A micropipette was used to remove the supernatant and keep the pellet as much as possible. The pellet was then resuspended with 500.0 μ L of sterile water. This process of centrifugation and removing of the supernatant was repeated. For each tube, either 200 μ L of experimental stock solutions was added or 200 μ L of sterile water was added as a control. Experimental and control groups were either subjected to 10 minutes of irradiation of visible light via the Rayonet photoreactor or covered and kept in dark for 10 minutes. After 10 minutes, the 700.0 μ L tubes were vortexed and 20.0 μ L of each sample was spread evenly over individual petri dishes containing LB agar. The plates were inverted then incubated at 28°C for 48 hours. The observed results reported are from

the effects of the multifunctional treatment composition or the individual components of the composition. These results are to visually, not quantitatively, see the effectiveness of the drug's inhibition of *E. coli* cells.

Fluorescence Studies of TMPyP in combination with DHN and Fe(III) ions.

Three different solution samples of 3 mL were prepared to study its fluorescence ability. The first sample contained only a solution of TMPyP which was prepared by mixing 18 μL of 1.0×10^{-3} M TMPyP with ultrapure water. The second solution composed of TMPyP, in combination with Fe(III) ions which was prepared by mixing 30 μL of 1.0×10^{-2} M iron (III) with 18 μL of 1.0×10^{-3} M TMPyP in ultrapure water. The last solution was prepared by mixing 36 μL of 1.0×10^{-2} M DHN and 18 μL of 1.0×10^{-3} M TMPyP in ultrapure water. Fluorescence emission was measured upon excitation of each solution at 423 nm with an excitation slit width of 10.0 nm and an emission slit width of 12.0 nm. Each experiment was carried out at room temperature and under normal atmospheric conditions.

The Optimization of Hydrogen Peroxide's Concentration by Oxidation of DHN.

Eight vials of equal amounts of TMPyP (6.0×10^{-6} M), Fe(III) ions (1.0×10^{-4} M), and DHN (1.2×10^{-4} M) solutions were prepared by mixing required amounts of TMPyP, Fe(III) ions, and DHN with ultrapure water at room temperature and under normal atmospheric conditions. Different micromolar (μM) amounts of H_2O_2 were added to each vial and was left in dark for about 3 minutes. A UV-vis spectrum was taken for each sample before the hydrogen peroxide was added and after 3 minutes of adding the

hydrogen peroxide. The oxidation of DHN was used as measure of finding the optimized concentration of hydrogen peroxide. The following concentrations of hydrogen peroxide were used to find the optimum concentration: 50 μM , 75 μM , 100 μM , 125 μM , 150 μM , 300 μM , 400 μM , and 500 μM .

Effects of DHN Oxidation by Optimized Hydrogen Peroxide and Varying Fe(III)

Ion Concentrations.

Seven vials of equal amounts of TMPyP (6.0×10^{-6} M), DHN (1.2×10^{-4} M), and H_2O_2 (400×10^{-6} M) were prepared by mixing required amounts of TMPyP, Fe(III) ions, DHN, and H_2O_2 with ultrapure water at room temperature and under normal atmospheric conditions. Various amounts of Fe(III) ions, ranging from 0.10 mM to 1.0 μM , was added to the solution and was left in the dark for about 3 minutes. A UV-vis spectrum was taken for each sample before the hydrogen peroxide was added and after 3 minutes of adding the hydrogen peroxide. The oxidation of DHN was used as a measure of finding the effects of varying the concentration of Fe(III) ions. For each of the eight solutions, the following concentrations of Fe(III) ions were added: 1.00×10^{-4} M, 2.25×10^{-5} M, 2.00×10^{-5} M, 1.75×10^{-5} M, 1.50×10^{-5} M, 1.00×10^{-5} M, and 1.00×10^{-6} M.

MCF-7 Cell Culture

MCF-7 cells were purchased from ATCC (American Type Culture Collection) and maintained in 5% DMSO at -80°C until needed for use. For culture, cells were maintained in RPMI 1460 Medium (Gibco, CA) enriched with 10% FBS (Fetal Bovine Serum) and 1% antibiotic/antimycotic at 37°C with 5% CO_2 in a humidified atmosphere.

Treatment of MCF-7 Cells

MCF-7 cells were seeded at 10,000 cells per well in a 96 well plate. Cells were left in a humidified atmosphere at 37°C with 5% CO₂ to attach for 24 hours. The cells were treated with 6.0×10^{-6} M of TMPyP, 1.2×10^{-4} M of DHN, and 1.0×10^{-4} of Fe(III) ions. There were also conditions of TMPyP and DHN, TMPyP and Fe, and TMPyP, DHN, and Fe. After treatment, the group of the cells was irradiated with visible light for 10 minutes using a Rayonet photoreactor. The other experimental group was not irradiated with visible light and was placed in a dark environment for 10 minutes.

Using MTS Assay for Determining Cell Viability

After treatment in visible light or dark conditions, a viability assay was carried out. Manufacturer's (Promega) instructions were followed. In short, 20 μ l of MTS solution was added to the media of each well and incubated for 4 hours. The plates were read at 492 nm using a SkanIt plate reader. This was also done after 24 and 48 hours of visible light or dark reactions.

CHAPTER 3

Results and Discussion

Generation of Singlet Oxygen ($^1\text{O}_2$), Hydroxyl radical ($\dot{\text{O}}\text{H}$), and Juglone by the Multifunctional Treatment Composition Through Visible Light Irradiation and Aerobic Conditions

To directly detect the generation of singlet oxygen ($^1\text{O}_2$) from TMPyP, a chemical called singlet oxygen sensor green (SOSG) was used. SOSG is a reagent used for detecting singlet oxygen and does not show response to other ROS such as hydroxyl radicals or superoxide anions. SOSG was added to an aqueous solution of TMPyP and was irradiated with visible light at 532 nm. In the presence of singlet oxygen, SOSG emits a green fluorescence. Figure 2 shows the fluorescence intensity of SOSG. With increased length of visible light irradiation, there is a gradual increase in the intensity of fluorescence which indicates the generation of singlet oxygen in aqueous solution.²³ Each spectrum shown in Figure 2 was recorded immediately after 10 minutes of irradiation with a 532 nm light which continued up to 60 minutes of irradiation. Figure 2b shows the emission intensity of SOSG at 525 nm which gradually increased after 60 minutes of irradiation with the 532 nm light. Additional similar experiments were conducted to ensure the presence of singlet oxygen. For example, the emissions intensity of SOSG

greatly increased in D₂O solvent compared to H₂O. In contrast, a physical singlet oxygen quencher, NaN₃, was used which showed that the fluorescence emission intensity significantly decreased. This data indicates that TMPyP is sufficient at generating singlet oxygen in an aqueous environment which suggests that TMPyP has capabilities of being a photosensitizer.

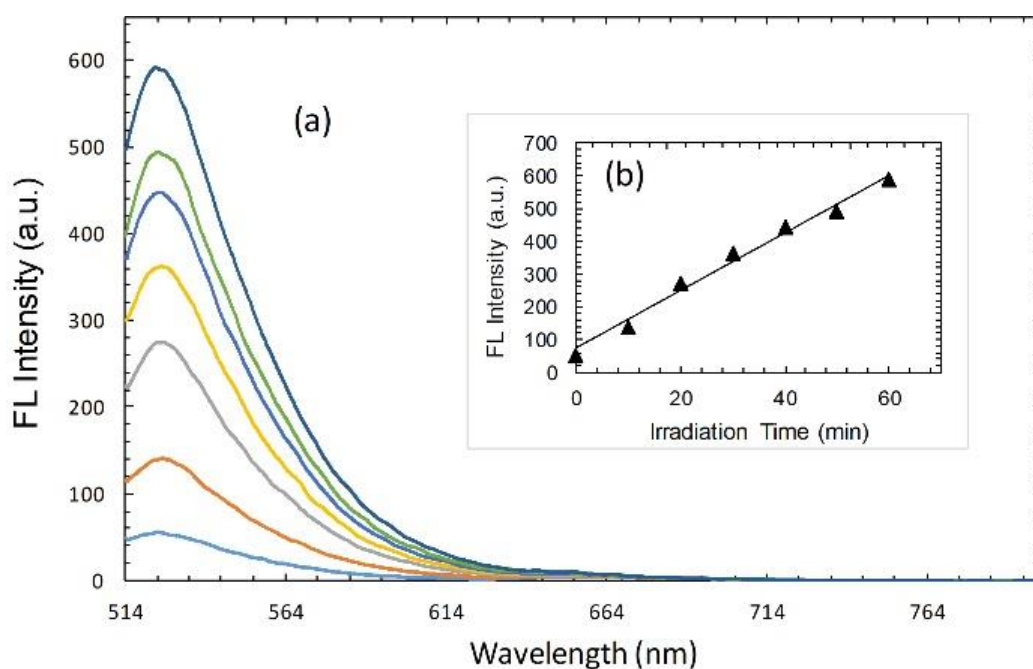
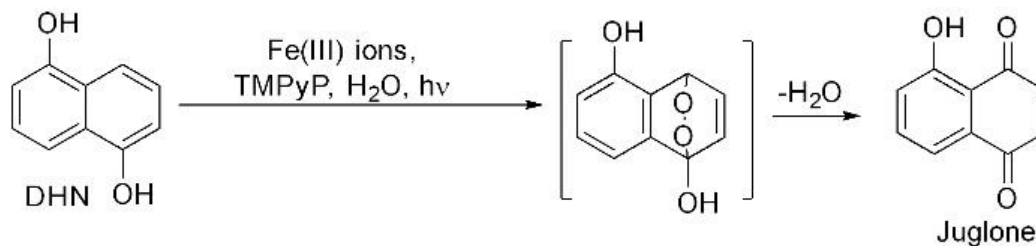


Figure 2: (a) The emissions plot for TMPyP (6.0×10^{-6} M) and SOSG in aqueous solution with a 532 nm laser for irradiation. Each curve represents length of irradiation with the laser: no irradiation time (blue); 10 minutes of irradiation (orange); 20 minutes (grey); 30 minutes (yellow); 40 minutes (light blue); 50 minutes (green); and 60 minutes (purple). (b) The SOSG peak at 525 nm after 60 minutes of irradiation by the 532 nm laser while recording the fluorescence spectra every 10 minutes. The following parameters for the spectrometer are as follows: Ex WL:423 nm; Start:433nm; End:800 nm; Ex Slit:10.0 nm; Em Slit:12.0 nm; Speed:1000 nm/min; Gain: High; Auto Lamp: on

TMPyP was also tested for its efficiency in generating singlet oxygen in an aqueous solution. Singlet oxygen quantum yield (Φ_{Δ}) was calculated by using methylene blue which has a known singlet oxygen yield of 0.52.²⁴ As a chemical probe to detect singlet oxygen in solution, 1,5-dihydroxynaphthalene (1,5-DHN) was used for the experiment. The reaction of 1,5-DHN and singlet oxygen is considered a fast reaction that forms Juglone as its primary product (Scheme 1).²⁵ The reaction is monitored by observing a steady decrease of the absorption of 1,5-DHN peaks at 295 nm to 355 nm. 1,5-DHN's ability as a singlet oxygen probe is needed for the singlet oxygen quantum yield measurement. Equation 1 shows how the singlet oxygen quantum yield was calculated for TMPyP.

$$\Phi_{\Delta(x)} = \Phi_{\Delta(s)} \times \frac{S_x}{S_s} \times \frac{F_s}{F_x} \quad Eq. 1$$

The S represents the slope of the plot of the absorbance vs irradiation and where F is the absorption correction factor. The singlet oxygen quantum yield of TMPyP was calculated to be 0.503. This value is lower than the 0.58 which was calculated by Gensch et al.²⁶ Other researchers have reported higher singlet oxygen quantum yields for TMPyP such as 0.74²⁷ and 0.9.²⁸



Scheme 1. The photooxidation of DHN to Juglone by reacting with singlet oxygen in the presence of TMPyP under visible light irradiation in aerobic conditions.

Scheme 1 depicts the photooxidation of 1,5-DHN by singlet oxygen to predominantly produce Juglone which is 5-hydroxy-1,4-naphthoquinone, a natural compound found in walnuts.^{25,29} Over the last few years, Juglone has been recognized for its pharmacological properties by possessing antibacterial and antitumor properties.³⁰ Additionally, Juglone has been characterized as a chemotherapeutic agent against cancers for its capability of inducing apoptosis to human breast cancer cells, colon cancer cells, and ovarian cancer cells.³¹ Figure 3 shows that upon irradiation of visible light to a solution of TMPyP and 1,5-DHN, there is a decrease in the absorption peaks at 301, 317, and 331 nm during the reaction. The decrease of the absorption of 1,5-DHN indicates that it was reacting with singlet oxygen and producing Juglone which is known to absorb around 423 nm. The Soret band of TMPyP and the absorption maximum of Juglone both appear at 420 nm²⁵ and 423 nm, respectively, which is why the increase of Juglone absorption at 423 nm is not observed upon irradiation of TMPyP and 1,5-DHN solution.

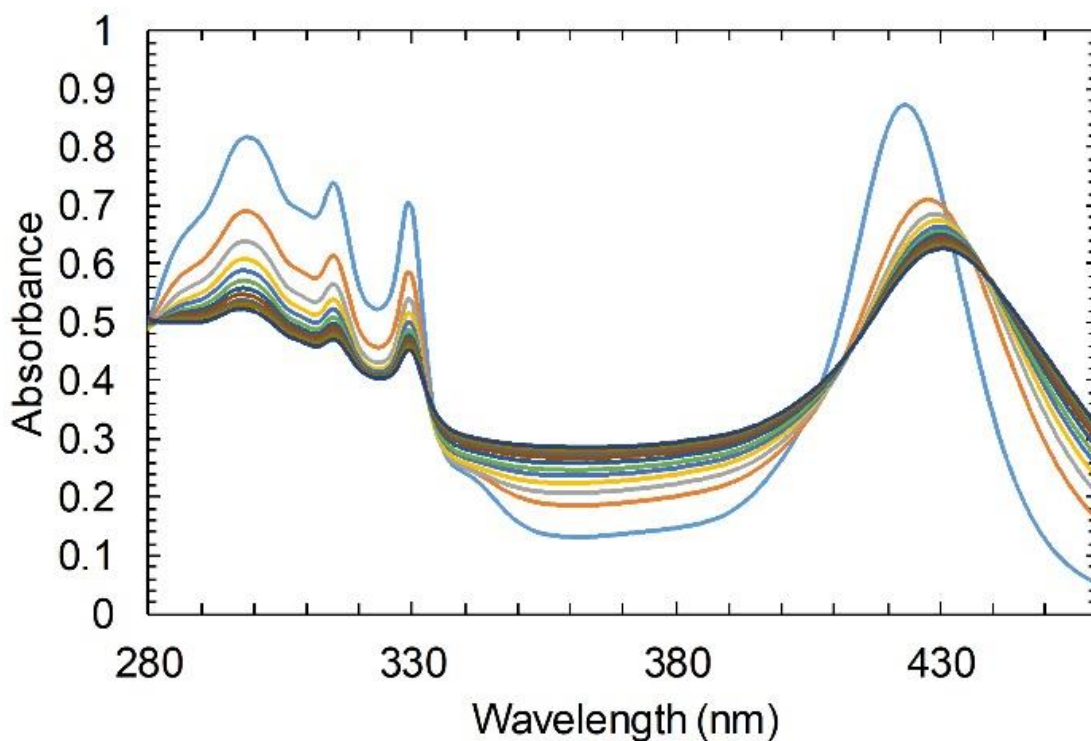


Figure 3: Photooxidation of DHN (1.2×10^{-4} M) by TMPyP (6.0×10^{-6} M) in aerobic aqueous solution. Absorptions measured at 0 minutes of irradiation (blue color line), 2 minutes (orange color line), 4 minutes (light grey color line), 6 minutes (yellow color line), 8 minutes (light blue color line), 10 minutes (green color line), 12 minutes (Navy blue color line), 14 minutes (maroon color line), 16 minutes (dark grey color line), 18 minutes (brown color line), and 20 minutes (teal color line) minutes.

Another component of the multifunctional solution is iron. As an essential nutrient in the human body, iron helps manage many functions which include metabolism, growth in mammalian cells, and playing a role in heme by binding oxygen to oxygenate tissues in the body. Conversely, iron is a transition metal which can accept or lose electrons and take part in free radical formation reactions.³² Iron was also studied for

its effects on the photooxidation of 1,5-DHN. Figure 4 portrays that the rate of photooxidation of 1,5-DHN by TMPyP was variable by the concentrations of Fe(III) ions in solution. The rate of photooxidation of 1,5-DHN by TMPyP, with various amounts of Fe(III) ions, was monitored at 301 nm and was observed to follow pseudo first order kinetics. The rate constants were calculated by linear regression fitting of the experimental data (calculated absorbance values as $\ln(A_0)/A$ vs t , where A_0 is the absorbance at time 0, and A is the absorbance at time (t)). The summary of all rate constants of the photooxidation of 1,5-DHN by TMPyP as a function of the concentration of Fe (III) ions is shown on Table 1. Without the presence of Fe (III) ions, the photooxidation of 1,5-DHN by TMPyP had a rate constant of $6.58 \times 10^{-4} \text{ s}^{-1}$. With the addition of 10 μL of $1.0 \times 10^{-3} \text{ M}$ Fe (III), the rate of the photooxidation of DHN did not initially increase ($k = 3.90 \times 10^{-4} \text{ s}^{-1}$) when compared to the metal free solution. However, increases to the rate were observed when additional amount of Fe(III) ions was added in increasing amounts. By the addition of 75 μL of $1.0 \times 10^{-2} \text{ M}$ of Fe(III) ions, the rate of photo-oxidation of 1,5-DHN by TMPyP reduced ($k = 5.68 \times 10^{-4} \text{ s}^{-1}$). Thus, to find an optimum concentration for Fe(III) ions, to be a component of the multifunctional solution with DHN ($1.2 \times 10^{-4} \text{ M}$) and TMPyP ($6.0 \times 10^{-6} \text{ M}$), a series of reactions were carried out with Fe (III) ion concentrations ranging from approximately 15 μL of $1.0 \times 10^{-2} \text{ M}$ to 50 μL of $1.0 \times 10^{-2} \text{ M}$. The maximum observed rate of photooxidation of 1,5-DHN by TMPyP was when Fe(III) ion concentration was about 50 μL of $1.0 \times 10^{-2} \text{ M}$ ($k = 9.43 \times$

10^{-4} s^{-1}). Thus, as a component of the multifunctional solution, $1.0 \times 10^{-4} \text{ M Fe(III)}$ would be used for all photooxidation studies.

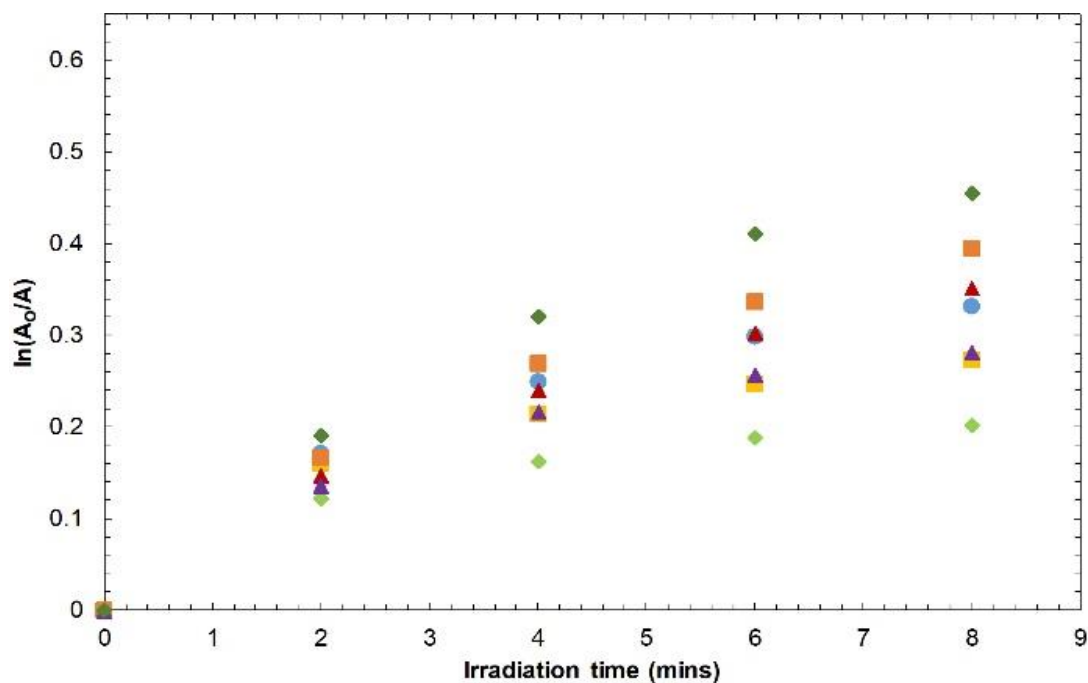


Figure 4: The calculated absorbance of DHN ($\ln(A_0)/A$) monitored at 301 nm as a function of irradiation time in the presence of DHN ($1.2 \times 10^{-4} \text{ M}$) and TMPyP ($6.0 \times 10^{-6} \text{ M}$) (blue circles); TMPyP ($6.0 \times 10^{-6} \text{ M}$), DHN ($1.2 \times 10^{-4} \text{ M}$), and Fe(III) ions ($1.0 \times 10^{-4} \text{ M}$) (dark green diamonds); TMPyP ($6.0 \times 10^{-6} \text{ M}$), DHN ($1.2 \times 10^{-4} \text{ M}$), and Fe(III) ions ($5.0 \times 10^{-5} \text{ M}$) (orange squares); TMPyP ($6.0 \times 10^{-6} \text{ M}$), DHN ($1.2 \times 10^{-4} \text{ M}$), and Fe(III) ions ($3.0 \times 10^{-5} \text{ M}$) (red triangles); TMPyP ($6.0 \times 10^{-6} \text{ M}$), DHN ($1.2 \times 10^{-4} \text{ M}$), and Fe(III) ions ($1.5 \times 10^{-4} \text{ M}$) (purple triangle); TMPyP ($6.0 \times 10^{-6} \text{ M}$), DHN ($1.2 \times 10^{-4} \text{ M}$), and Fe(III) ions ($4.0 \times 10^{-6} \text{ M}$) (yellow square); and TMPyP ($6.0 \times 10^{-6} \text{ M}$), DHN ($1.2 \times 10^{-4} \text{ M}$), and Fe(III) ions ($2.0 \times 10^{-6} \text{ M}$) (light green diamonds) in aerobic aqueous solution.

Table 1. Summary of rate constants of DHN photo-oxidation by TMPyP as a function of [Fe (III) ions] in aerobic conditions.

Solution of DHN and TMPyP with	Rate Constant, k_{obs} (s^{-1})	R^2
No Fe (III) ions	6.58×10^{-4}	0.8951
2.0×10^{-6} M Fe (III)	3.90×10^{-4}	0.8321
4.0×10^{-6} M Fe (III)	5.27×10^{-4}	0.8507
3.0×10^{-5} M Fe (III)	7.15×10^{-4}	0.9505
5.0×10^{-5} M Fe (III)	7.98×10^{-4}	0.9495
1.0×10^{-4} M Fe (III)	9.43×10^{-4}	0.9422
1.5×10^{-4} M Fe (III)	5.68×10^{-4}	0.9018

With all three components of the multifunctional solution, an effort to find the nature of produced ROS was made by carrying out a series of control reactions. Similar to previous experiments, Figure 5 shows the photooxidation of 1,5-DHN by TMPyP/Fe(III) ions and was found to be increased dramatically in D_2O solvent compared to H_2O which indicates the presence of singlet oxygen. However, for these sets of experiments, a Rayonet photoreactor was used instead of a laser. Again, a significantly slower photooxidation 1,5-DHN by TMPyP/Fe(III) ions was observed in the presence of a physical quencher of singlet oxygen, NaN_3 .

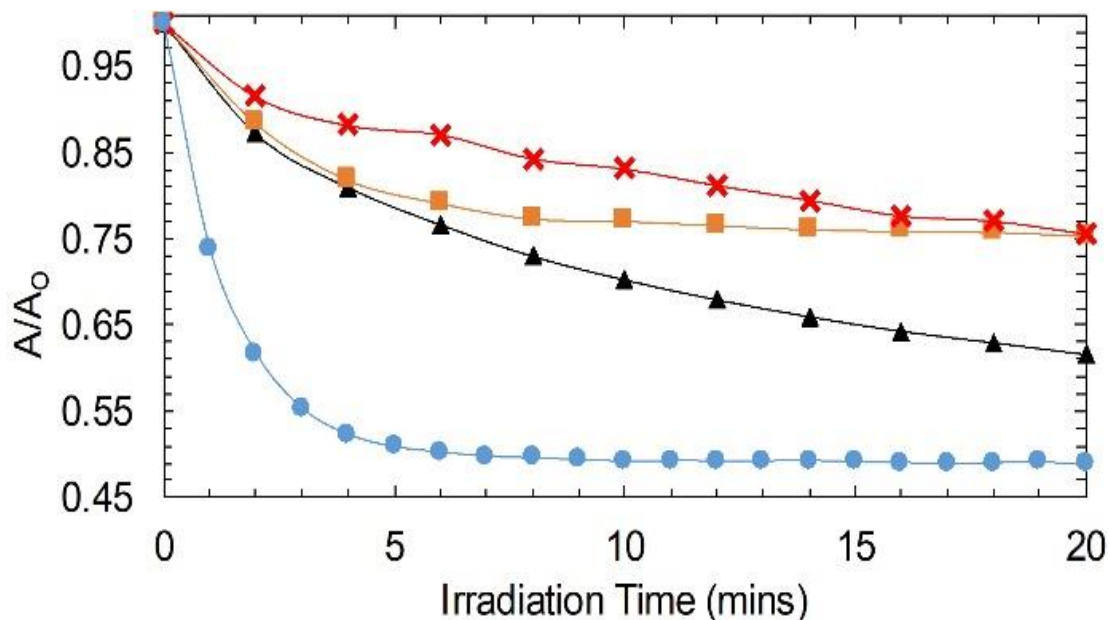


Figure 5: The rate of change of DHN monitored at 301 nm as a function of irradiation time. Experiments were conducted in the presence of DHN (1.2×10^{-4} M), TMPyP (6.0×10^{-6} M), and NaN_3 (100 mM) (Red cross); DHN (1.2×10^{-4} M), TMPyP (6.0×10^{-6} M), and D_2O (Blue circle); DHN (1.2×10^{-4} M), TMPyP (6.0×10^{-6} M), and Iron (1.0×10^{-4} M) (orange square); and DHN (1.2×10^{-4} M), TMPyP (6.0×10^{-6} M), and H_2O (Black triangle)

Although singlet oxygen seemed to be the prime ROS, experiments were carried out to determine if hydroxyl radicals ($\dot{\text{O}}\text{H}$) could also be photooxidizing 1,5-DHN by TMPyP/Fe (III) ions. These experiments were carried out in the presence of a hydroxyl radical quencher, 2-propanol. Studies have indicated that 2-propanol reacts very quickly hydroxyl radicals ($1.3 \times 10^{-9} \text{ M}^{-1}\text{s}^{-1}$)³³ and produces 2-propanone as a product which can be detected by GC-MS spectrometry³⁴. A series of experiments were carried out with an excess of 2-propanol to verify the production of hydroxyl radical. The photooxidation of 1,5-DHN by TMPyP/Fe (III), in the presence of 2-propanol, was qualitatively analyzed

through GC-MS data which indicated that the photo-induced generation of ROS was able to convert 2-propanol to its principal oxidation product, 2-propanone in the presence of 1,5-DHN. Further experimentation showed that without the presence of 1,5-DHN, the TMPyP/Fe(III) solution was incapable of producing 2-propanone in the presence of visible light which indicated that 1,5-DHN needed to be present. This data shows that with all three components of the multifunctional solution present, it can form singlet oxygen and hydroxyl radicals in an aqueous solution, with visible light irradiation, and aerobic condition.

Since iron can be present in different oxidation states and also be covalently bonded to the core of a porphyrin ring, a few experiments were carried out to test the photooxidation effects of 1,5-DHN by TMPyP and different irons. Figure 6 shows a comparison of the rates of the photooxidation of 1,5-DHN by TMPyP/Fe(III), TMPyP/Fe(II), and Fe(III)TMPyP (where the iron is covalently bonded to the center of porphyrin ring) in an aqueous and aerobic condition. Table 2 contains the rate constants for each experiment and they are as follows: $2.2 \times 10^{-5} \text{ s}^{-1}$ for TMPyP with Fe(II), $5.5 \times 10^{-5} \text{ s}^{-1}$ for Fe(III)TMPyP, and $1.1 \times 10^{-4} \text{ s}^{-1}$ for TMPyP with Fe(III) ions. TMPyP and Fe(III) ions shows a rate that is 2 times faster than Fe(III)TMPyP. With all things considered, Fe (III)/1,5-DHN/TMPyP has shown characteristics for being a potential therapeutic solution which is capable of producing singlet oxygen, hydroxyl radicals, and Juglone or its derivatives under visible light and aerobic conditions. These special characteristics can be applied to superficial cancer treatments or cancers where the target

is able to be irradiated with visible light and has the presence of molecular oxygen. In addition, the formation of Juglone and its derivatives from the multifunctional solution also possesses anticancer and antimicrobial activity²⁹ which can potentially kill target cells as well.

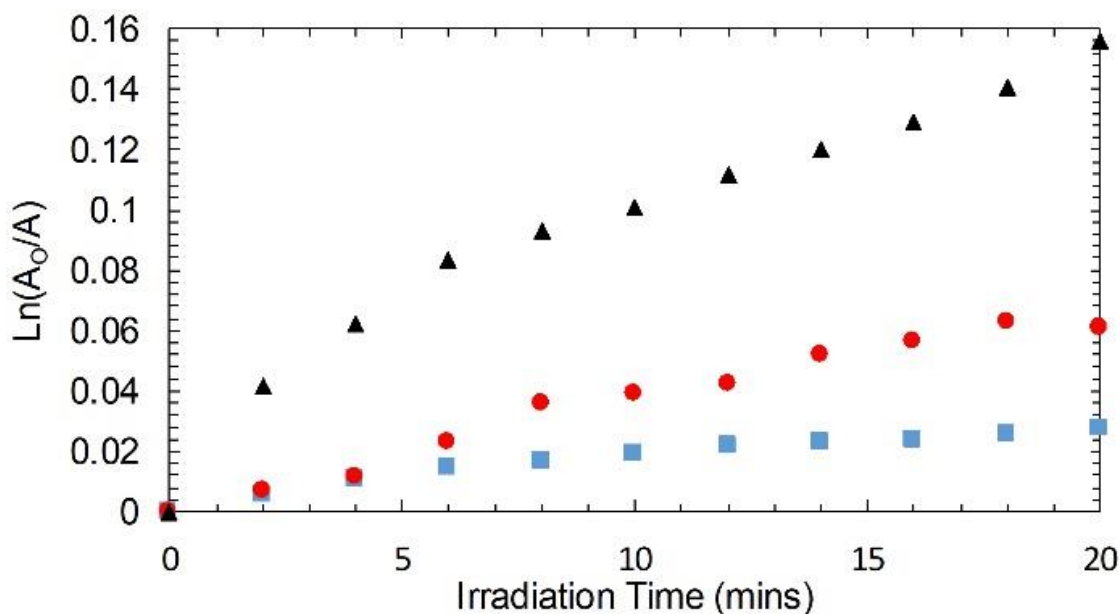


Figure 6: The rate of change for DHN (1.2×10^{-4} M) peak at 301 nm when irradiated with 20 minutes of light in solutions with Fe(III)TMPyP (6.0×10^{-6} M) (blue square); TMPyP (6.0×10^{-6} M) and iron (II) (1.0×10^{-4} M) (red circle); and TMPyP (6.0×10^{-6} M) and iron (III) (1.0×10^{-4} M) (black triangle) in aerobic, aqueous solution.

Table 2: Rates of photooxidation of DHN (1.2×10^{-4} M) monitored at 301 nm as a function of irradiation time in the presence of Fe TMPyP (6.0×10^{-6} M), TMPyP (6.0×10^{-6} M) and iron (II) (1.0×10^{-4} M), and TMPyP (6.0×10^{-6} M) and iron (III) (1.0×10^{-4} M), respectively, in aerobic aqueous solution. k_{obs} is the rate constant (s^{-1}) of the DHN decay kinetics.

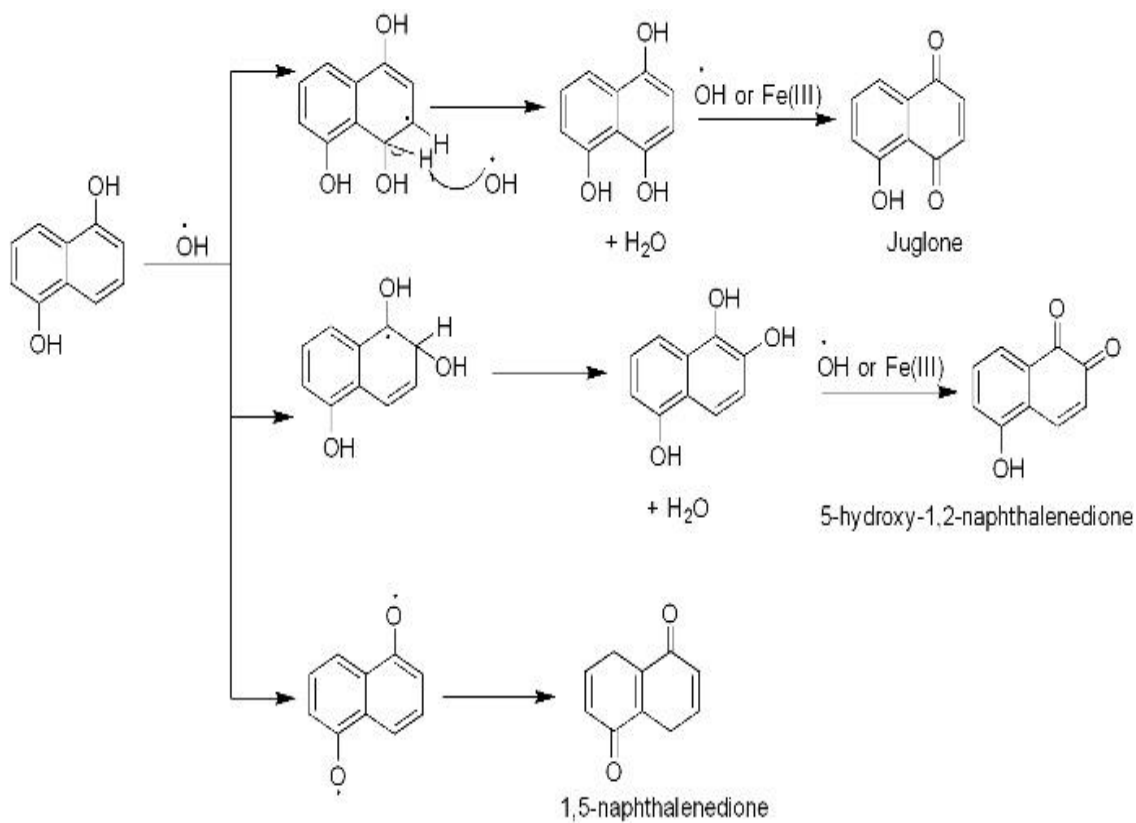
Solution of DHN with	Rate Constant, k_{obs} (s^{-1})	R^2
Fe TMPyP	5.5×10^{-5}	0.9679
TMPyP and Iron (II)	2.2×10^{-5}	0.9329
TMPyP and Iron (III)	1.1×10^{-4}	0.9342

Generation of Hydroxyl radical ($\dot{O}H$) and Juglone by the Multifunctional solution in Anaerobic Condition with Visible Light Irradiation.

Since tumor hypoxia poses as a threat to the effectiveness of PDT, the multifunctional solution was tested for its ability to generate ROS in anaerobic conditions. Prior literature shows that for porphyrins with metals such as Fe(III) and Mn(III), covalently bonded to the core of the porphyrin, have to capability to undergo a photoreduction process to generate hydroxyl radicals in aqueous solution.³⁵ Although the mechanism is not well understood, Equation 2 shows the possible intramolecular rearrangement for the generation of hydroxyl radicals by Fe(III) and Mn(III) porphyrins under light conditions.



To determine if the multifunctional solution could produce hydroxyl radicals in anaerobic conditions, Fe(III)/1,5-DHN/TMPyP was thoroughly purged with argon and irradiated with visible light. For continuity, this solution was also compared to Fe(II)/1,5-DHN/TMPyP and Fe(III)TMPyP (where the iron is covalently bonded to the center of porphyrin ring) to determine if a difference in iron can affect the reaction. The absorption of 1,5-DHN at 301 nm was recorded every 2 minutes to monitor its degradation. Scheme 2 depicts a proposed reaction of how 1,5-DHN could interact with hydroxyl radicals to produce Juglone or its derivatives.³⁶ Figure 7 shows the comparison rates of photooxidation of 1,5-DHN by TMyP/Fe(III), TMPyP/Fe(II), and Fe(III)TMPyP in anaerobic aqueous conditions. Similar to aerobic conditions, the photooxidation of 1,5-DHN by TMPyP/Fe(III) ($k = 1.12 \times 10^{-4} \text{ s}^{-1}$) was approximately two times faster when compared to the Fe(III)TMPyP solution ($k = 5.50 \times 10^{-5} \text{ s}^{-1}$). Moreover, the rate of photooxidation for 1,5-DHN was observed to be approximately five times slower in the TMPyP/Fe(II) solution ($k = 2.17 \times 10^{-5} \text{ s}^{-1}$) when compared to TMPyP/Fe(III).



Scheme 2. The proposed reactions of hydroxyl radicals and DHN with the formation of Juglone and Juglone derivatives.

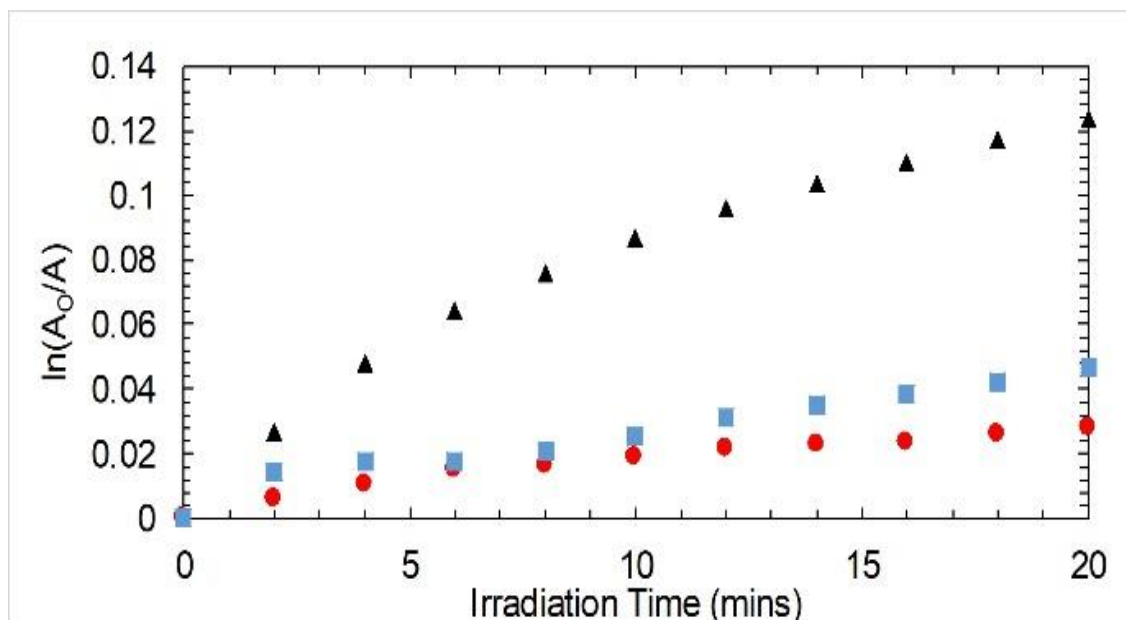


Figure 7: The rate of change for DHN (1.2×10^{-4} M) peak at 301 nm when irradiated with 20 minutes of light in solutions with Fe(III)TMPYP (6.0×10^{-6} M) (blue square); TMPYP (6.0×10^{-6} M) and iron (II) (1.0×10^{-4} M) (red circle); and TMPYP (6.0×10^{-6} M) and iron (III) (1.0×10^{-4} M) (black triangle) in anaerobic, aqueous solution.

Again, similar to the aerobic condition, the concentration of Fe(III) ions was varied to study its influence on the photooxidation of 1,5-DHN, but now in anaerobic conditions. As shown on Figure 8, 1,5-DHN showed negligible photooxidation when Fe(III) ions were absent in the TMPyP solution. Unlike the aerobic condition, this data indicated that TMPyP alone is not able to produce ROS in anaerobic conditions and even when irradiated with visible light. However, with Fe(III) ions present with TMPyP, there is clear evidence of photooxidation of 1,5-DHN without the presence of oxygen. Figure 9 shows the rate of changes of the photooxidation of 1,5-DHN by TMPyP in various different concentrations of Fe(III) ions. For these experiments, the degradation of the

absorption of 1,5-DHN was observed to obey pseudo first order decay kinetics, so the rate constants were calculated from the slope of the experimental data (calculated absorbance values as $\ln(A_0)/(A)$ vs t , where A_0 is the absorbance at time 0, and A is the absorbance at time t). Table 3 shows a summary of the rate constants for each trial of varying concentrations of Fe(III). The maximum rate ($1.90 \times 10^{-4} \text{ s}^{-1}$) was achieved upon addition of 50 μL of $1.0 \times 10^{-2} \text{ M}$ of Fe(III). However, upon addition of 75 μL of $1.0 \times 10^{-2} \text{ M}$ of Fe (III) ions ($k = 1.13 \times 10^{-4} \text{ s}^{-1}$), the rate constant of the photooxidation of 1,5-DHN began to slow down in solution

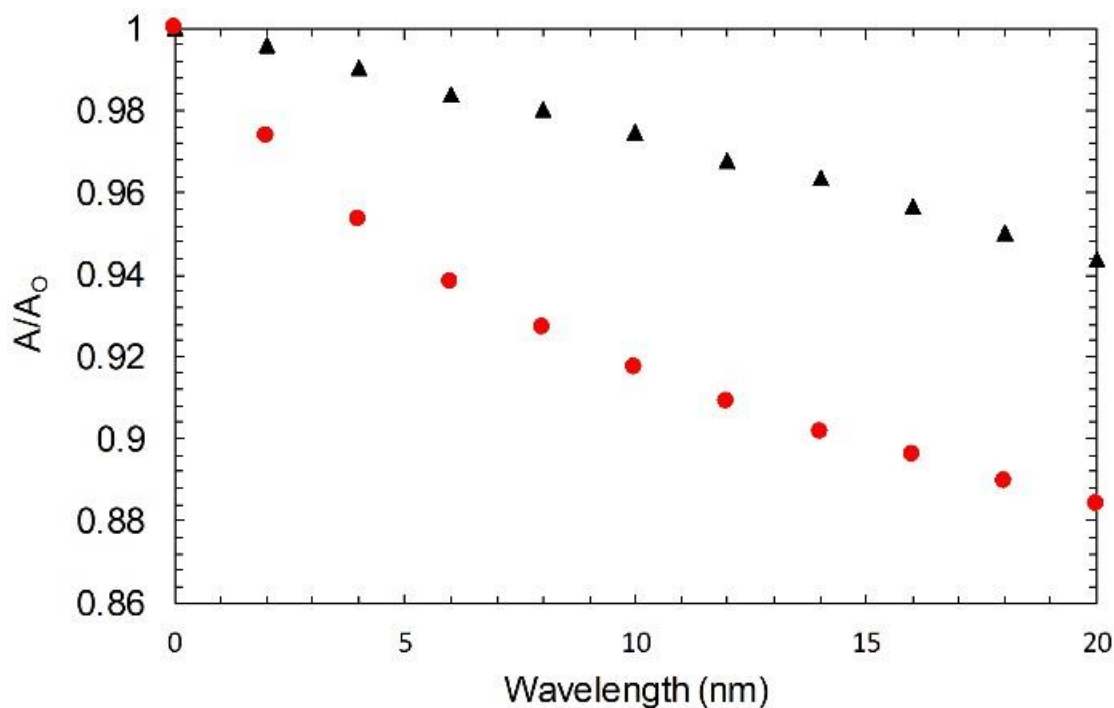


Figure 8: The change in the absorbance peak (301 nm) of DHN ($1.20 \times 10^{-4} \text{ M}$) in an anaerobic aqueous solution of just TMPYP ($6.0 \times 10^{-6} \text{ M}$) (black triangle) and an anaerobic aqueous solution of TMPYP ($6.0 \times 10^{-6} \text{ M}$) and iron (III) ($1.0 \times 10^{-4} \text{ M}$) (red circle)

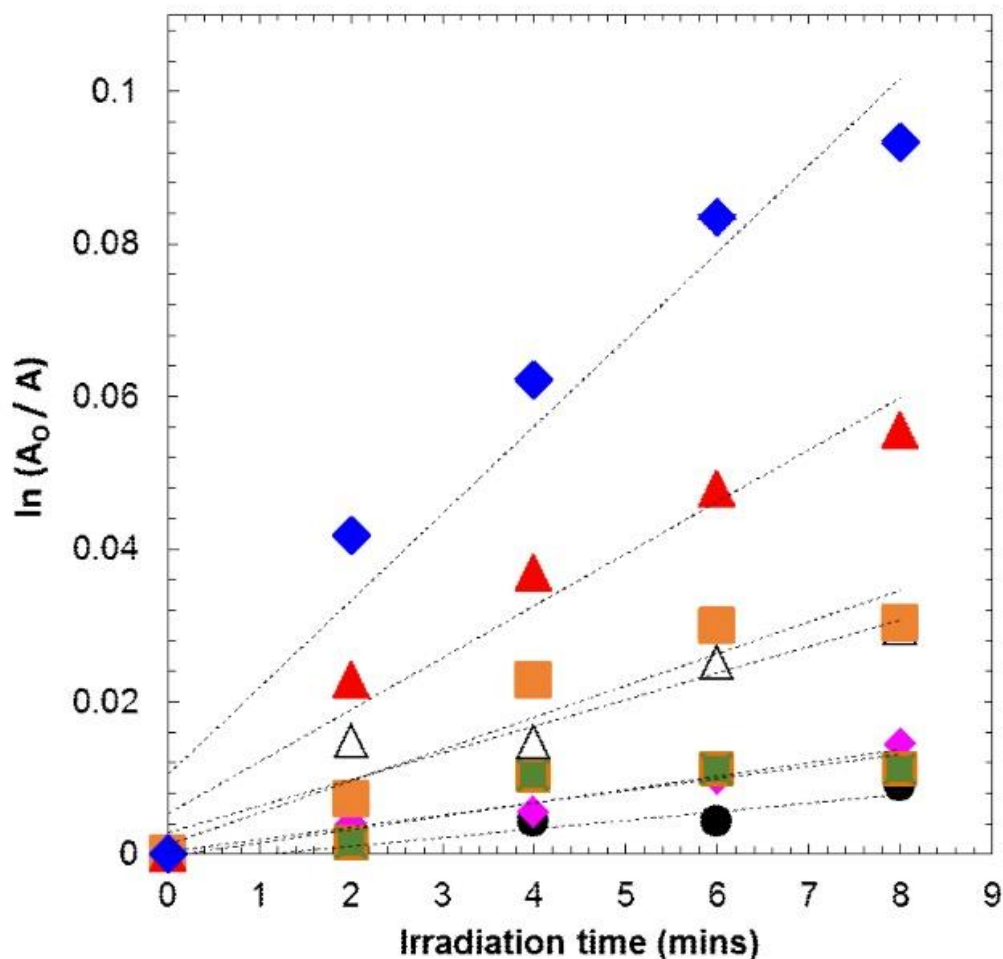


Figure 9: The calculated absorbance of DHN ($\ln(A_0)/A$) monitored at 301 nm as a function of irradiation time in the presence of DHN (1.2×10^{-4} M) and TMPyP (2.8×10^{-6} M) (black circles); TMPyP (6.0×10^{-6} M), DHN (1.2×10^{-4} M), and Fe(III) ions (2.0×10^{-6} M) (purple diamonds); TMPyP (6.0×10^{-6} M), DHN (1.2×10^{-4} M), and Fe(III) ions (4.0×10^{-6} M) (green squares); TMPyP (6.0×10^{-6} M), DHN (1.2×10^{-4} M), and Fe(III) ions (3.0×10^{-5} M) (empty triangles); TMPyP (6.0×10^{-6} M), DHN (1.2×10^{-4} M), and Fe(III) ions (5.0×10^{-5} M) (orange squares); TMPyP (6.0×10^{-6} M), DHN (1.2×10^{-4} M), and Fe(III) ions (1.0×10^{-4} M) (blue diamonds); and TMPyP (6.0×10^{-6} M), DHN (1.2×10^{-4} M), and Fe(III) ions (1.5×10^{-4} M) (red triangles) in anaerobic aqueous solution.

Table 3. Summary of all the rate constants for the photooxidation of DHN by TMPyP as a function of [Fe (III) ions] in anaerobic conditions.

Solution of DHN and TMPyP with	Rate Constant, k_{obs} (s^{-1})	R^2
No Fe (III) ions	1.80×10^{-5}	0.8642
2.0×10^{-6} M Fe (III)	2.80×10^{-5}	0.9783
4.0×10^{-6} M Fe (III)	2.70×10^{-5}	0.8177
3.0×10^{-5} M Fe (III)	5.80×10^{-5}	0.9221
5.0×10^{-5} M Fe (III)	7.00×10^{-5}	0.9169
1.0×10^{-4} M Fe (III)	1.90×10^{-4}	0.9434
1.5×10^{-4} M Fe (III)	1.13×10^{-4}	0.9579

To confirm that the ROS being produced were hydroxyl radicals, a series of control reactions for the multifunctional solution were carried out in when irradiated with visible light in anaerobic conditions. The first experiment consisted of purging Fe(III)/1,5-DHN/TMPyP with argon and testing for its capability of generating oxygen gas, which was monitored by an oxygen meter, for more than two hours of irradiation with visible light. This experiment showed no sign of oxygen gas production, so there is no possibility for the ROS to be singlet oxygen because its production requires the presence of oxygen. Even with the presence of a photosensitizer and visible light, there could not be any production of singlet oxygen. Therefore, the ROS is believed to be something other than singlet oxygen. To further verify the absence of singlet oxygen, similar photosensitization experiments were carried out in D_2O solvent. When compared to the experiment using H_2O as the solvent, there was no evidence of an increase in the rate of photooxidation of 1,5-DHN.

With no singlet oxygen present in anaerobic conditions, the next possible ROS that was tested for was hydroxyl radicals. Similar 1,5-DHN photooxidation reactions were carried out in an anaerobic environment using TMPyP/Fe(III) ions and in the presence of excess 2-propanol. Qualitative GC-MS analysis indicated that 2-propanol was converted to 2-propanone as an oxidized product. Interestingly, like previous results, no 2-propanone was detected by GC-MS analysis when the argon purged solution did not contain 1,5-DHN. Again this data indicated that all three components, 1,5-DHN/TMPyP/Fe(III), must be present for the production of hydroxyl radicals in anaerobic aqueous environment. The discovery that the multifunctional solution has the ability to produce hydroxyl radicals in anaerobic conditions is remarkable and may serve as a new PDT treatment option for hypoxic tumors.

Detoxification of H₂O₂ with Production of Hydroxyl Radicals and Juglone by Multifunctional Solution in the Absence of Visible Light.

Producing ROS without the presence of visible light is a major limitation of PDT since photosensitizers depend on visible light to convert dissolved oxygen to singlet oxygen. PDT is ineffective when tumors are deep in the body and light delivery systems have difficulty reaching the organ/tissue. Moreover, if the tumor is too large, then the light delivery systems also face the challenge of not being strong enough to penetrate the tumor. Since tumor cells are often hypoxic, another issue for PDT therapy is the lack of oxygen available to create singlet oxygen. Fenton reactions utilizing Fe(II) in the

presence of hydrogen peroxide have been shown to produce hydroxyl radicals without irradiation of visible light. Therefore, hydrogen peroxide was added to the multifunctional solution to test its ability to produce hydroxyl radicals in a Fenton-like reaction. Like other experiments, different oxidation states of iron were used, as well as iron that was coordinated to the center of TMPyP's porphyrin ring. Figure 10 shows the oxidation of 1,5-DHN by TMPyP/Fe(III), TMPyP/Fe(II), and Fe(III)TMPyP with increasing microliter amounts of hydrogen peroxide under dark conditions. Specifically, a higher rate of 1,5-DHN is observed with TMPyP/Fe(III) and Fe(III)TMPyP when compared to the TMPyP/Fe(II) ions. Scheme 3a presents a standard Fenton-like reaction where hydrogen peroxide reacts with Fe(III) ions and forms a Fe(III)-peroxo complex that later decomposes into Fe(II) and hydroperoxyl radicals. This produced Fe(II) ions can further react with hydrogen peroxide to generate hydroxyl radicals through a standard Fenton reaction (Scheme 3b). Interestingly, the produced hydroperoxyl radicals can react with the following: Fe(III) ions, Fe(II) ions, or other hydroperoxyl radicals to produce oxygen gas and Fe(II), Fe(III)-peroxo complex, or oxygen gas alone, respectively.³⁷ This aspect of the Fenton and Fenton-like reactions could be extremely advantageous for treating cancer cells. Although these preliminary results require the addition of hydrogen peroxide to be effective in dark conditions, reports in literature have shown that cancer cells produce more hydrogen peroxide than normal cells due to their characteristics of abnormal cellular proliferation.³⁸ Normally, an enzyme called catalase has the vital protective role of preventing the buildup of hydrogen peroxide by converting it to water

and oxygen.³⁸ However, physiological concentrations of catalase are not sufficient enough to detoxify the increased amounts of hydrogen peroxide produced which has been shown to leave many cells without efficient protection and can actually increase the progression of cancer cells.³⁹⁻⁴⁰ Remarkably, this reaction of the multifunctional composition with hydrogen peroxide suggests that the Fenton-like reaction can generate hydroxyl radicals and, at the same time, oxidize 1,5-DHN without the presence of visible light to form Juglone or its derivatives. In addition, oxygen gas that is produced from these Fenton-like reactions could also play a role in eliminating hypoxic environments which will help increase the effectiveness of PDT. As a control, 1,5-DHN with TMPyP showed no oxidation with increased concentrations of hydrogen peroxide. In addition, 1,5-DHN alone showed no observable signs of being oxidized in the presence of hydrogen peroxide. This data suggest that Fe(III) ions and hydrogen peroxide are the required reagents for the generation of hydroxyl radicals in aqueous solution.

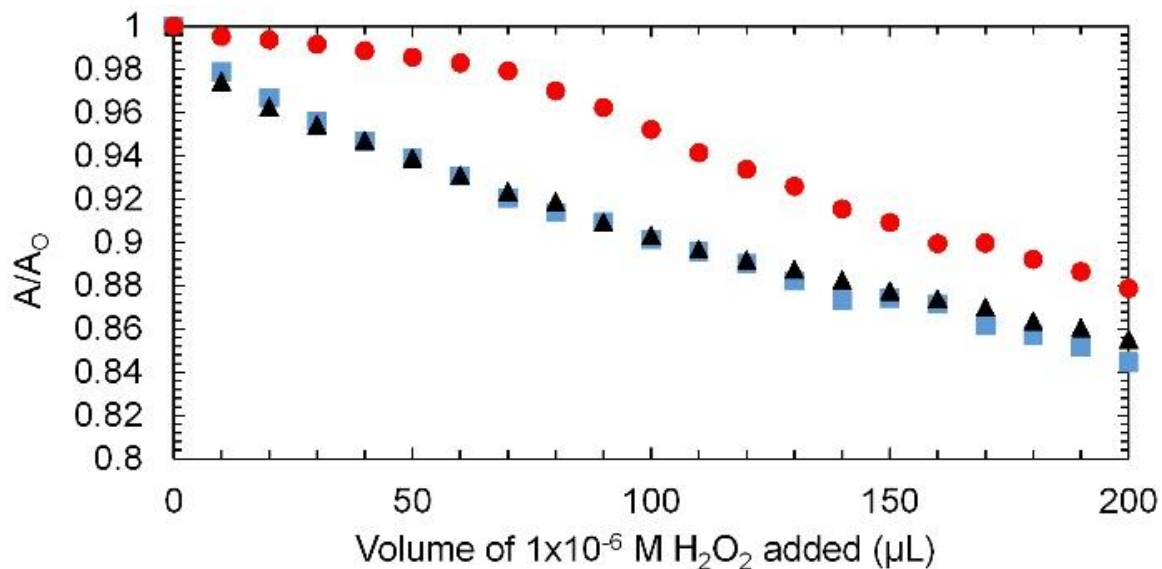


Figure 10: The rate of change for DHN (1.2×10^{-4} M) peak at 301 nm when 1.0×10^{-6} M H_2O_2 is added to the solution of Fe(III)TMPYP (6.0×10^{-6} M) (blue square); TMPYP (6.0×10^{-6} M) and iron (II) (1.0×10^{-4} M) (red circle); and TMPYP (6.0×10^{-6} M) and iron (III) (1.0×10^{-4} M) (black triangle) in aerobic, aqueous solution under dark conditions.

To improve the benefits of the Fenton-like reaction for producing hydroxyl radicals in aqueous and dark conditions, an experiment was implemented to determine an optimum concentration for hydrogen peroxide and Fe(III) ions. Figure 11a is an experiment where the concentrations of 1,5-DHN (1.2×10^{-4} M), TMPyP (6.0×10^{-6} M), and Fe(III) (1.0×10^{-4} M) were kept constant and varying amounts of hydrogen peroxide were added. Figure 11a shows that a maximum decrease in the absorption of 1,5-DHN, at 301 nm, was observed when 400 μ M of hydrogen peroxide was added. In addition, Figure 11b shows the difference in the absorption of 1,5-DHN when in the presence of 50

μM and $400 \mu\text{M}$ of hydrogen peroxide which were the lowest and optimal concentrations tested, respectively.

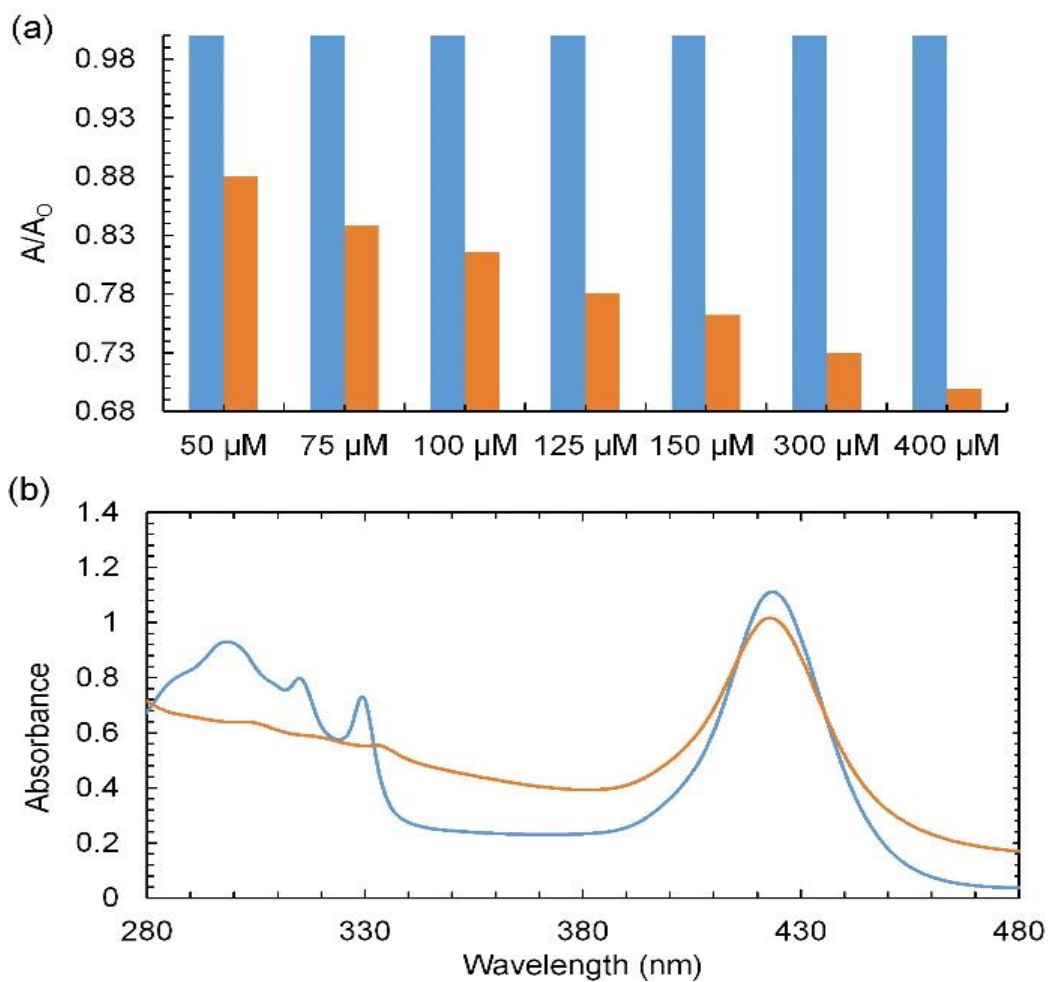


Figure 11: (a) Optimization of H_2O_2 concentration in the presence of $1 \times 10^{-4} \text{ M}$ iron (III) in aerobic, aqueous solution under dark conditions. (b) The UV-vis spectra of the recorded optimum H_2O_2 concentration at $400 \mu\text{M}$.

In contrast, a similar experiment was carried out to find the optimum concentration of Fe(III) ions by varying its concentration when TMPyP, 1,5-DHN, and hydrogen peroxide (400 μM) are kept constant. Figure 12a depicts the changes in the absorption of 1,5-DHN at 301 nm with varying concentrations of Fe(III) ions. In this figure, there is a maximum decrease in 1,5-DHN's absorption when a concentration of 25 μM is used for Fe(III) ions (see Figure 12b for full spectrum of 1,5-DHN's oxidation in presence of 25 μM of Fe(III) ions).

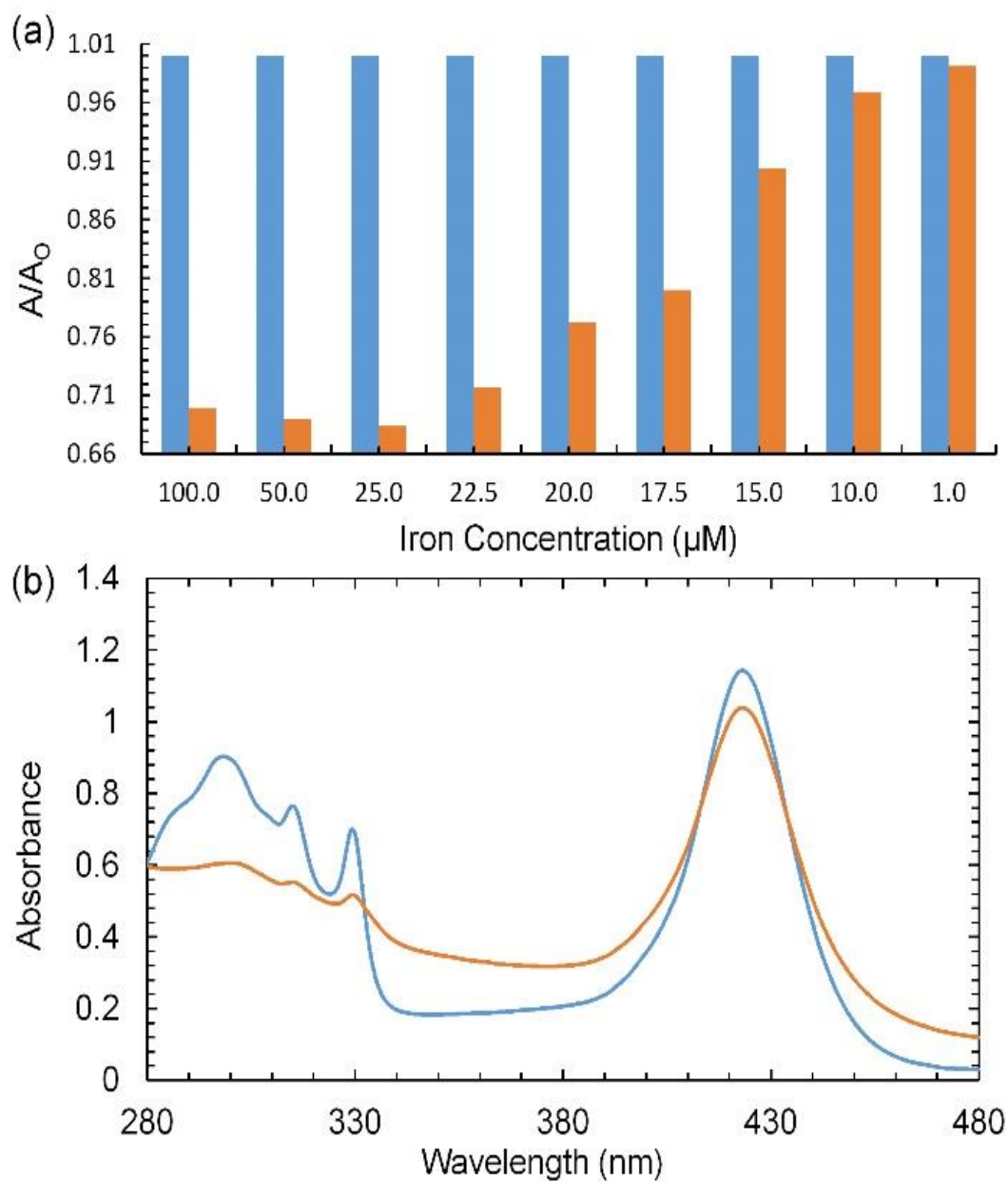


Figure 12: (a) Optimization of iron (III) concentration in the presence of 400 μM iron (III) in aerobic, aqueous solution under dark conditions. (b) The UV-vis spectra of the recorded optimum iron (III) concentration at 25.0 μM .

To our surprise, when higher concentrations of Fe(III) ions (1.0×10^{-2} M) and hydrogen peroxide (1.0×10^{-2} M) were used with TMPyP and 1,5-DHN, oxygen gas bubbles could be visually observed in the solution at room temperature under normal atmospheric conditions (Figure 13a). This visual generation of oxygen gas was confirmed using an oxygen meter and was found to be dependent on high concentrations of Fe(III) and hydrogen peroxide, as previous experiments did not produce oxygen gas that could be seen visually. Interestingly, when Fe(III)TMPyP was placed in high concentrations of hydrogen peroxide, there was brown sludge precipitate of Fe(OH)₃ which was not present in the Fe(III)/1,5-DHN/TMPyP mixture (Figure 14). For each experiment, the pH before and after the experiment was recorded. The pH of the solution would begin at 5.5 and gradually decrease to 3.0 upon addition of hydrogen peroxide. This change in pH suggests that, upon reaction of Fe(III) with hydrogen peroxide, oxygen gas is produced with a release of protons into the solution as described previously on Scheme 3b. In short, it appears that the multifunctional treatment composition has the capability of detoxifying excess hydrogen peroxide to oxygen gas which can partially help alleviate hypoxic environments and potentially decrease the progression of cancer cells. Moreover, without the presence of visible light, the multifunctional treatment solution can still produce hydroxyl radicals and Juglone and its derivatives to potentially kill cancer cells (Scheme 3c).

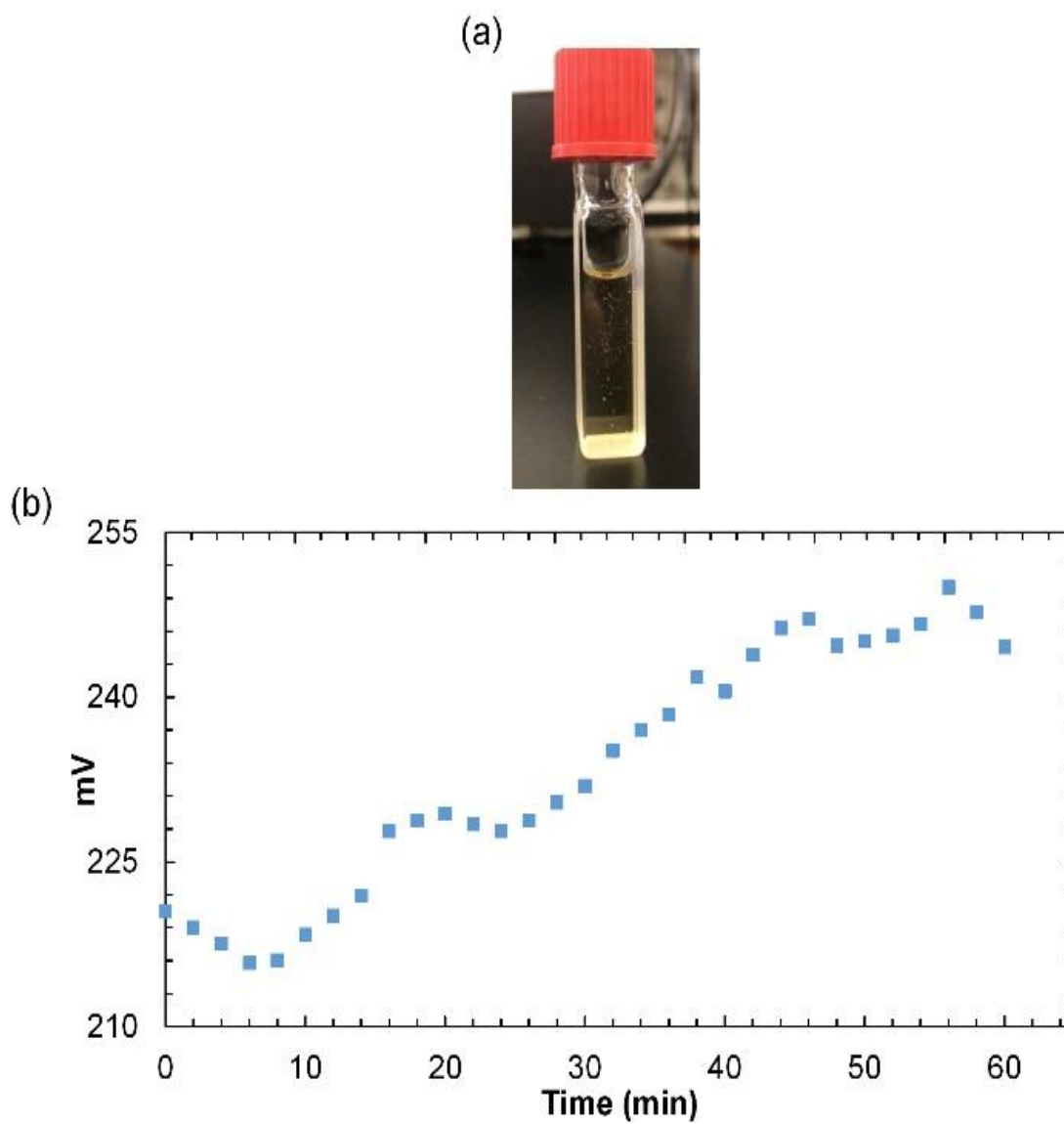


Figure 13: (a) Oxygen gas generation in an aqueous iron (III) (1.0×10^{-2} M) and H_2O_2 (1.0×10^{-2} M).; (b) Oxygen gas measured by oxygen electrode in mV vs time (min).

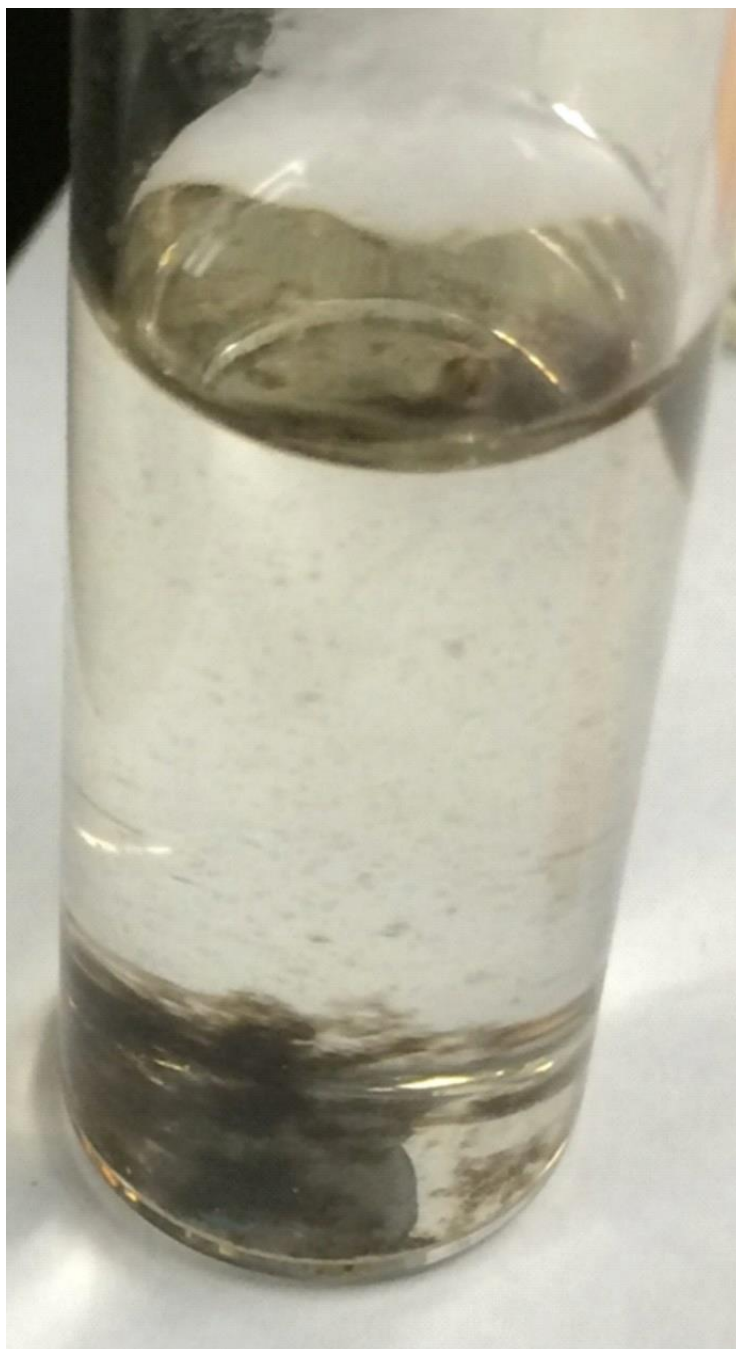
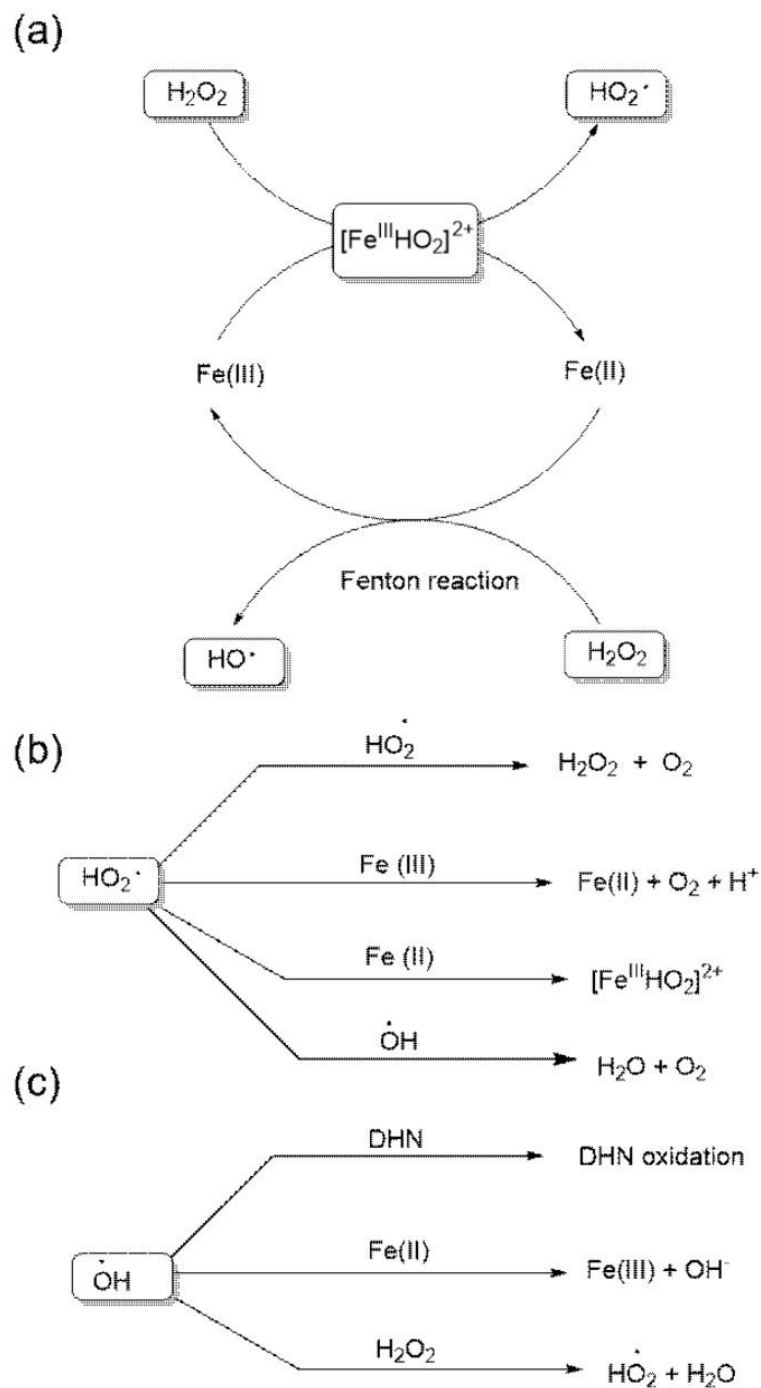


Figure 14: Dark precipitate in solution with Fe TMPyP (5.71×10^{-6} M), DHN (1.14×10^{-4} M) and H_2O_2 (1.0×10^{-1} M) after 18 hours.



Scheme 3. (a) Possible reactions from Fenton-like reaction, (b) possible reactions from HO_2^\bullet , and (c) possible reactions from OH^\bullet .

Fluorescence Study of the Multifunctional Treatment Composition and its Components.

Figure 15 depicts the emission spectra of TMPyP in aqueous solution which has a maximum at 657 nm when excited at 423 nm. Several experiments were carried out to determine how the intensity of TMPyP changes with the addition of the Fe(III) ions and 1,5-DHN. When the Fe(III) ions were added to the TMPyP solution, the fluorescence intensity of the solution showed negligible changes. However, with the addition of 1,5-DHN to the TMPyP and Fe(III) ions mixture, there appeared to be a slight decrease to the intensity.

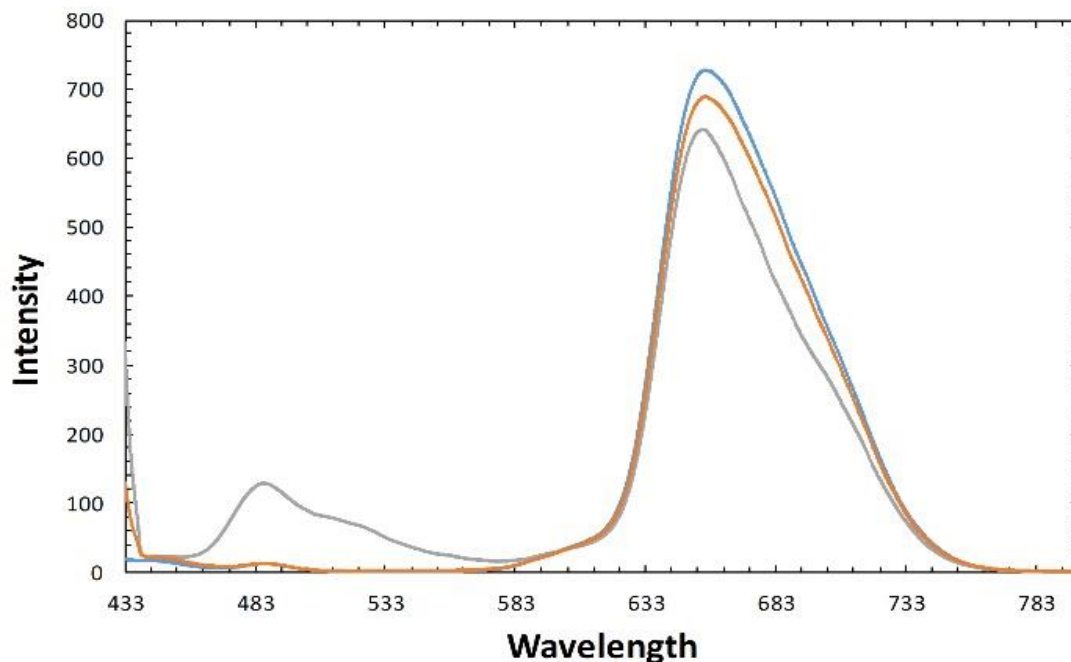


Figure 15. Emission spectra for TMPyP, iron (III), and DHN in aqueous solution. The blue line is 6.0×10^{-6} M TMPyP alone. The orange line is 6.0×10^{-6} M TMPyP with 1.0×10^{-4} M iron (III). The grey line is 6.0×10^{-6} M TMPyP, 1.0×10^{-4} M iron (III), and 1.2×10^{-4} M DHN. Each sample recorded was ran using the following parameters: Ex WL:423 nm; Start:433 nm; End:800 nm; Ex Slit:10.0 nm; Em Slit:12.0 nm; Speed:1000 nm/min; Gain: High; Auto Lamp: on

The fluorescence quantum yield (Φ_F) of TMPyP was calculated using Equation 3 while crystal violet (1.0×10^{-5} M) was used as a standard with a known fluorescence quantum yield of 0.020 in water.⁴¹

$$\Phi_{F(x)} = \Phi_{F(s)} \times \frac{A_s}{A_x} \times \frac{F_x}{F_s} \times \left(\frac{n_x}{n_s}\right)^2 \quad \text{Eq. 3}$$

For this equation, A represents the absorbance, while F represents the area under the emission's curve, and where n is the refractive index of the solvent used. Upon calculation, the fluorescence quantum yield of TMPyP was observed to be 0.0139.

Current literature shows the fluorescence quantum yield to be 0.016.⁴² This data indicates that TMPyP can fluoresce in aqueous media with only minor decreases to its fluorescence intensity when Fe(III) ions and 1,5-DHN is present.

***In vitro* effects of the Multifunctional Treatment Composition, Under Visible Light Irradiation, on BL21 *E. coli* in Aerobic Conditions.**

The first stage of *in vitro* cell growth studies included testing the multifunctional solution on *E. coli* bacteria to determine its efficacy in stopping or slowing the progression of *E. coli* cell growth as a treatment composition. Several trials with various chemical combinations were conducted. Table 4 shows the survival of *E. coli* when treated with (a) 1,5-DHN, (b) Juglone, (c) TMPyP/Fe(III), (d) TMPyP/1,5-DHN, and (e) TMPyP/1,5-DHN/Fe(III) ions in the absence and presence of light.

Table 4. Survival of *Escherichia coli* in the presence of DHN, Juglone, Fe (III), and TMPyP with various combinations.

Solution	Dark (%)	Light (%)
Control	3.8×10^6 (100)	3.8×10^6 (100)
DHN	3.8×10^6 (100)	820 (<0.01)
Juglone	130 (<0.01)	2 (<0.01)
TMPyP + Fe(III)	3.8×10^6 (100)	41 (<0.01)
TMPyP + DHN	143 (<0.01)	0 (0)
TMPyP + DHN + Fe(III)	221 (<0.01)	0 (0)
TMPyP + Juglone + Fe(III)	26 (<0.01)	0 (0)

Figure 16a shows the experimental trial of 1,5-DHN (1.2×10^{-4} M) in the absence and presence of light which showed no inhibition (0 %) of growth of *E. coli*. Since Juglone is the photooxidized product of 1,5-DHN and is also known for its antibacterial and anticancer activity, Juglone was tested against *E. coli* which can be seen on Figure 16b.^{29,43} This data shows that Juglone has complete inhibition (99.99 %) of growth when treated in dark or in the presence of visible light. Figure 16c shows a solution of TMPyP/Fe(III) ions which showed 0 % inhibition of growth in *E. coli* cells during dark conditions. This specific chemical combination suggests that it is non-toxic to the *E. coli* cells when not irradiated with visible light. However, in the presence of visible light, there was near complete inhibition (~100 %) of *E. coli* growth (Figure 16c). This data is clear that reactive oxygen species, mainly singlet oxygen, is produced from the photosensitization of TMPyP. Similarly, 100 % inhibition of growth was observed when TMPyP/1,5-DHN was reacted with *E. coli* solution under visible light, and interestingly this solution showed significant inhibition (~99.99 %) in the absence of light (Figure 16d). The mechanism for how TMPyP/1,5-DHN inhibits *E. coli* cells in dark is not quite well understood. Finally, the multifunction treatment composition, TMPyP/1,5-DHN/Fe(III) ions, was tested against the *E. coli*. In the presence of light and absence of light, the multifunctional treatment composition showed a complete inhibition (100 %) of growth and significant inhibition (~99 %), respectively. Lastly, since the oxidized product of 1,5-DHN is Juglone, a separate experiment was carried out to determine if TMPyP/Juglone/Fe(III) ions could slow or stop *E. coli* cell growth. Figure 16f shows that

there is a complete inhibition of *E. coli* growth when this treatment is in the presence of light and without light. In short, this data suggests that TMPyP/1,5-DHN/Fe(III) solution can produce ROS and Juglone or its derivatives which can be used to kill *E. coli* cells in the presence of visible light. Furthermore, the multifunctional solution is a promising solution that can potentially stop or slow the progressions of *E. coli*.

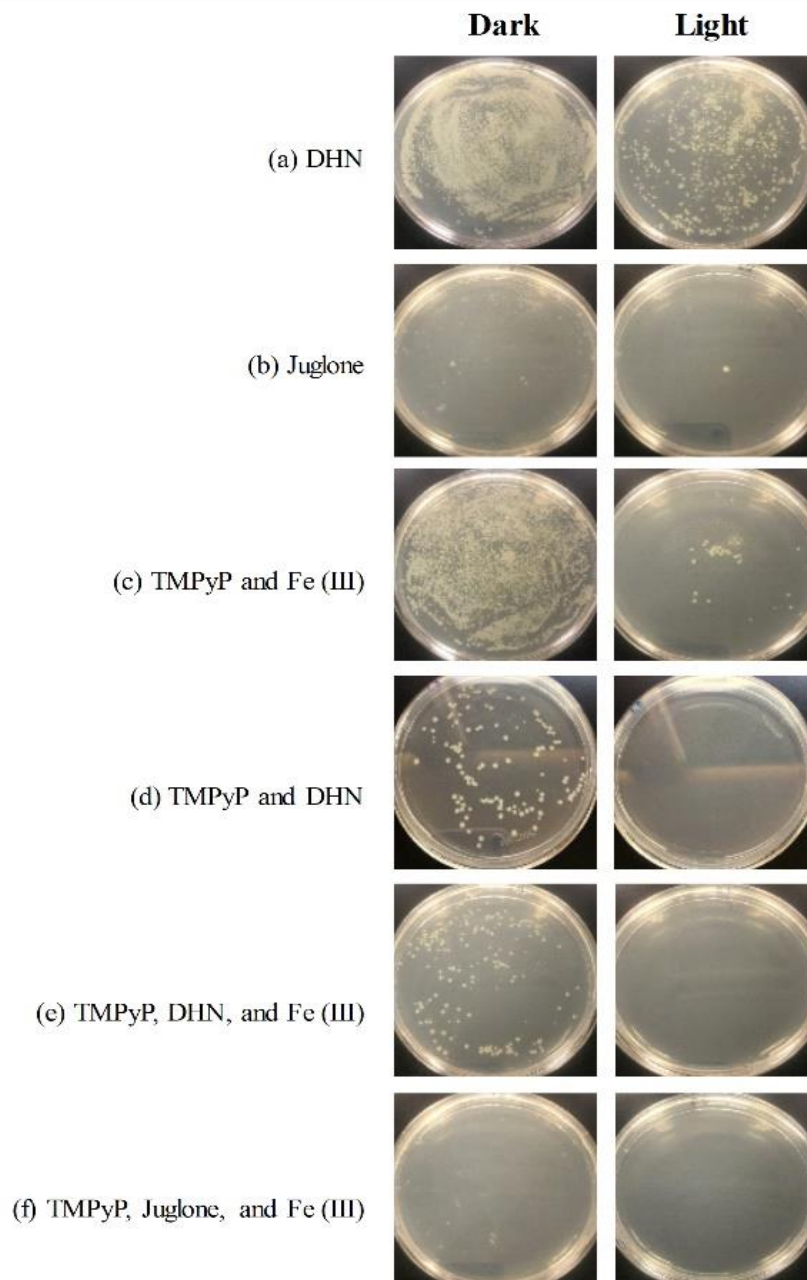


Figure 16. *E. coli* growth monitored after 48 hours, with (a) 1.2×10^{-4} M DHN (b) 1.2×10^{-4} M Juglone (c) 6.0×10^{-6} M TMPyP and 1.0×10^{-4} M Fe (III) (d) 6.0×10^{-6} M TMPyP and 1.2×10^{-4} M DHN (e) 6.0×10^{-6} M TMPyP, 1.2×10^{-4} M DHN, and 1.0×10^{-4} M iron (III) (f) 6.0×10^{-6} M TMPyP, 1.2×10^{-4} M Juglone, and 1.0×10^{-4} M iron (III).

***In vitro* effects of the Fenton-like reactions on BL21 *E. coli* in the Absence of Visible Light.**

The first stage of *in vitro* studies was expanded by including hydrogen peroxide rich environments to determine if it has potential to be effective against *E. Coli* cells and be part of the multifunctional treatment composition's unique characteristics. As stated previously in Scheme 3a, in Fenton-like reactions, Fe(III) ions and hydrogen peroxide can produce ROSs such as hydroxyl radicals and hydroperoxyl radicals. Since these ROS are known for killing bacteria such as *E. Coli*, the Fenton-like reactions were examined. In particular, *E. Coli* was mixed with hydrogen peroxide in dark conditions and in room temperature. Figure 17 depicts a significant inhibition of growth of *E. coli* when 1.0×10^{-4} M Fe(III) ions and 400 μ M H₂O₂ were used together. As a control, Fe(III) ions at a concentration of 1.0×10^{-4} M and 1.0×10^{-3} M Fe(III) was used alone to determine if it was toxic to the *E. Coli* cells. In similar fashion, 400 μ M of hydrogen peroxide alone was also used as a control. In short, there was no inhibition of growth in the bacteria when the Fe(III) ions and hydrogen peroxide were administered alone. However, when 400 μ M of hydrogen peroxide and 1.0×10^{-3} M Fe(III) were used, the results showed nearly a complete inhibition of *E. Coli*. These observations indicate that the multifunctional treatment solution will be able to produce ROS and kill bacteria and potentially cancer cells in dark when hydrogen peroxide is present.

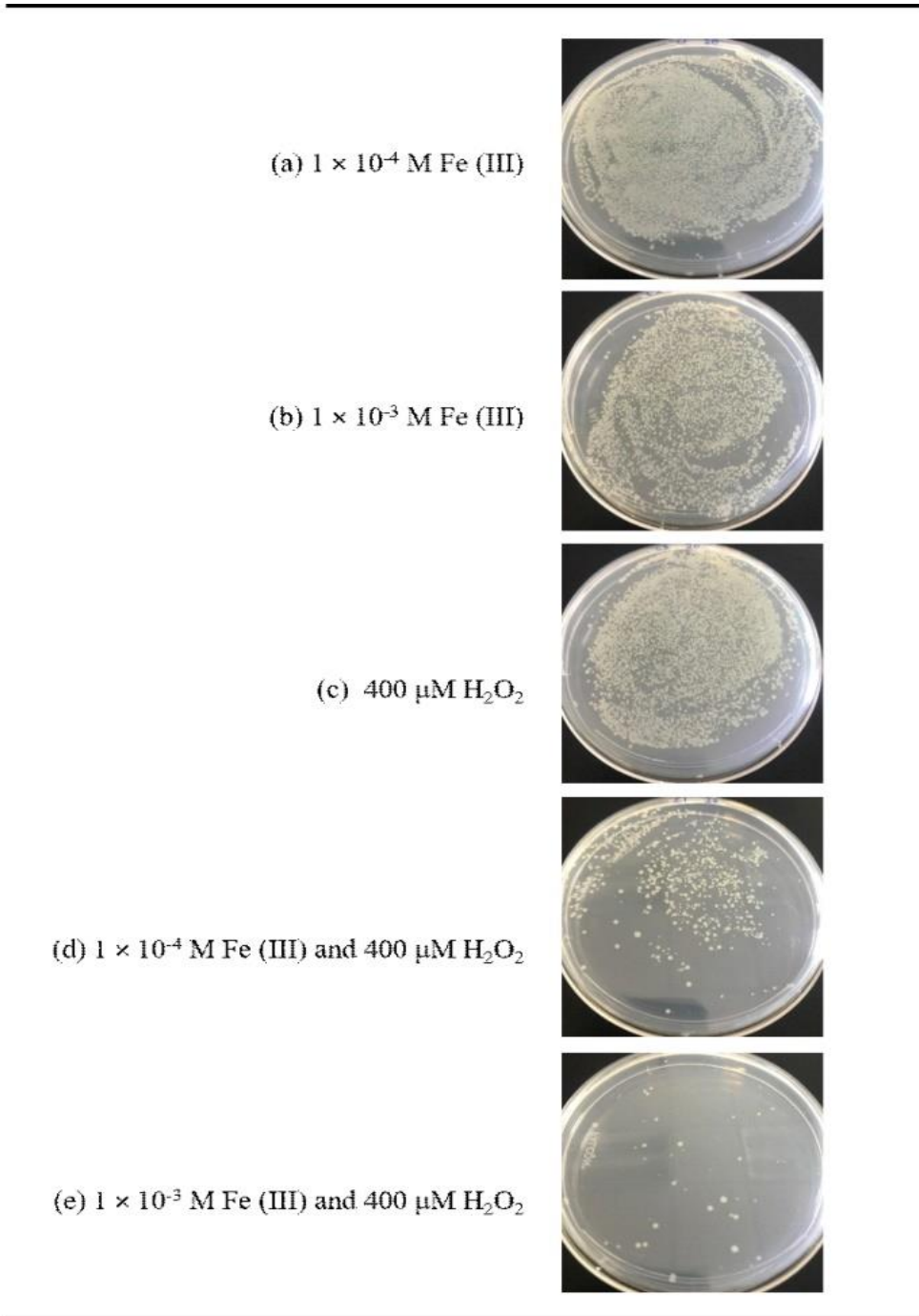


Figure 17: *E. coli* growth, monitored after 48 hours, with (a) 1×10^{-4} M Fe (III) (b) 1×10^{-3} M Fe (III) (c) 400 μ M H_2O_2 (d) 1×10^{-4} M Fe (III) and 400 μ M H_2O_2 (e) 1×10^{-3} M Fe (III) and 400 μ M H_2O_2 .

***In vitro* effects of the Multifunctional Treatment Composition on MCF-7 Breast Cancer Cells.**

The positive results from the *E. Coli* experiments led to a new set of experiments which was to test the multifunctional treatment solution on MCF-7 breast cancer cells. Approximately 10,000 cells/well were treated with a combination of TMPyP at 6.0×10^{-6} M, 1,5-DHN at 1.2×10^{-4} M, and Fe(III) ions at 1.0×10^{-4} M under normal room temperature and pressure. Table 5 shows a summary, in percentage, of MCF-7 cell survival after being treated with a single dose of the multifunctional treatment solution. For each experiment, the cells were either exposed to visible light or left in dark for 10 minutes. TMPyP alone is capable of producing singlet oxygen in the presence of visible light and was able to kill 22 % of MCF-7 cells when irradiated by visible light. In contrast, in dark, TMPyP was only able to kill approximately 1.6 % of the cells (Table 5). Through the presence of Fe(III) ions alone, there was approximately 4 % inhibition of MCF-7 cells with visible light present. Lastly, with 1,5-DHN present alone with visible light, there was nearly 13 % of inhibition of cell growth. However, when all components were added together there was a considerable amount of inhibition, approximately 52 %, when the composition was in the presence of visible light for about 10 minutes. When the concentration of the treatment composition increased, there was an increase in inhibition of cell growth. These results indicated that the treatment composition was dose dependent. Moreover, a separate experiment showed that if the treatment did not continue

after 10 minutes of visible light irradiation, then the cells were able to grow back and divide within 24 to 48 hours.

Table 5. Percent survival of 10,000 MCF-7 cells in 10 minutes of light and dark condition where each trial's cell viability was measured immediately after treatment.

Sample	Light (%)	Dark (%)
Control	95.97	92.01
Acetonitrile	104.03	107.99
TMPyP	74.18	98.43
DHN	83.09	98.92
Fe ³⁺	91.53	103.00
TMPyP + Fe ³⁺	67.33	95.60
TMPyP + DHN	51.09	91.28
TMPyP + Fe ³⁺ + DHN	44.81	88.74

In contrast, similar experiments were carried out but in the absence of visible light to determine if there were any therapeutic effects of the multifunctional treatment solution on MCF-7 breast cancer cells. Similar to the visible light results, the three components, TMPyP, Fe(III) ions, and 1,5-DHN, were used separately and showed little to no inhibition of growth when in the absence of visible light. Interestingly, when all components were placed together, there was only minimal cell death, approximately 3 %, when compared to the control in dark. More investigation and additional repeats of the experiments are needed to further confirm these results. However, it is possible that the cancer cells contained a low concentration of hydrogen peroxide which only produced minimal ROS or Juglone and its derivatives to treat the cells which could explain why there was only slight inhibition of cell growth.

CHAPTER 4

Conclusion

In conclusion, the multifunctional treatment solution is comprised of TMPyP, 1,5-DHN, and Fe(III) ions. Each component has a specific role and is pertinent for overcoming several limitations of PDT. In an aerobic environment, TMPyP is able to produce singlet oxygen, hydroxyl radicals, and Juglone or its derivatives under visible light irradiation. The addition of Fe(III) ions were shown to increase the rate of photooxidation of 1,5-DHN when compared to the addition of Fe(II) ions and Fe(III) coordinated to the porphyrin ring. Under anaerobic conditions, TMPyP alone is only minimally able to photooxidize 1,5-DHN. Without the presence of oxygen, singlet oxygen is unable to be generated which poses as a major limitation for PDT. However, with the addition of Fe(III) ions, the photooxidation of 1,5-DHN is observed and is faster than Fe(II) ions and Fe(III)TMPyP where Fe(III) is coordinated to the center of the porphyrin. Moreover, Fenton-like reactions were utilized because the Fe(III) component of the multifunctional treatment solution has the ability to react with hydrogen peroxide that is produced from cancer cells. An optimum concentration of 25 μM Fe(III) reacted with 400 μM hydrogen peroxide to produce hydroxyl radicals, Juglone, and oxygen gas (O_2) in the absence of visible light and without forming $\text{Fe}(\text{OH})_3$ sludge. This remarkable

ability has potential to treat tumors that are unable to be penetrated, deep in tissues, by visible light which is another limitation of PDT. In addition to the multifunctional treatment solution's potential in anticancer ability, this treatment solution also has potential in containing antibacterial properties. The composition was observed to inhibit the growth of *E. coli* in the presence of light, hydrogen peroxide, and dark conditions. Lastly, we investigated the treatment solution against MCF-7 breast cancer cells *in vitro* and observed that the solution can partially inhibit the growth of breast cancer cells. However, further studies and experimentations are needed against a variety of cancer cell lines to observe the true potential of the multifunctional treatment composition.

REFERENCE

1. Kudinova, N. V.; Berezov, T. T., *Biochemistry (Moscow) Supplement Series B: Biomedical Chemistry* **2010**, 4 (1), 95-103.
2. Dougherty, T. J.; Gomer, C. J.; Henderson, B. W.; Jori, G.; Kessel, D.; Korbelik, M.; Moan, J.; Peng, Q., *Journal of the National Cancer Institute* **1998**, 90 (12), 889-905.
3. Sharman, W. M.; Allen, C. M.; van Lier, J. E., *Drug Discovery Today* **1999**, 4 (11), 507-517.
4. Luo, J.; Solimini, N. L.; Elledge, S. J., *Cell* **2009**, 136 (5), 823-837.
5. Busch, T. M.; Hahn, S. M.; Evans, S. M.; Koch, C. J., *Cancer Research* **2000**, 60 (10), 2636-2642.
6. Tromberg, B. J.; Orenstein, A.; Kimel, S.; Barker, S. J.; Hyatt, J.; Nelson, J. S.; Berns, M. W., *Photochemistry and Photobiology* **1990**, 52 (2), 375-385.
7. Foster, T. H.; Murant, R. S.; Bryant, R. G.; Knox, R. S.; Gibson, S. L.; Hilf, R., *Radiation Research* **1991**, 126 (3), 296-303.
8. aR. Baskaran, J. Lee, S.-G. Yang, *Biomaterials Research* **2018**, 22, 25; bA. I. F. dos Santos, D. R. Q. de Almeida, L. F. Terra, M. c. S. Baptista, L. Labriola, *Journal of Cancer Metastasis and Treatment* **2019**, 5; cT. J. Dougherty, C. J. Gomer, B. W. Henderson, G. Jori, D. Kessel, M. Korbelik, J. Moan, Q. Peng, *JNCI: Journal of the National Cancer Institute* **1998**, 90, 889-905; dD. Kessel, *Photochemistry and Photobiology*, n/a.

9. A. Garcia-Sampedro, A. Tabero, I. Mahamed, P. Acedo, *Journal of Porphyrins and Phthalocyanines* **2019**, 23, 11-27.
10. A. Villanueva, J. C. Stockert, M. Cañete, P. Acedo, *Photochemical & Photobiological Sciences* **2010**, 9, 295-297.
11. Lainé, A.-L.; Passirani, C., *Current Opinion in Pharmacology* **2012**, 12 (4), 420-426.
12. Lennicke, C.; Rahn, J.; Lichtenfels, R.; Wessjohann, L. A.; Seliger, B., *Cell Communication and Signaling* **2015**, 13 (1), 39.
13. Kabel, A. M., *World Journal of Nutrition and Health* **2014**, 2 (3), 35-38.
14. Torti, S. V.; Torti, F. M., *Nat Rev Cancer* **2013**, 13 (5), 342-355.
15. Dizdaroglu, M.; Rao, G.; Halliwell, B.; Gajewski, E., *Archives of Biochemistry and Biophysics* **1991**, 285 (2), 317-324.
16. Dizdaroglu, M.; Jaruga, P., *Free Radical Research* **2012**, 46 (4), 382-419
17. Qiang, Z.; Chang, J.-H.; Huang, C.-P., *Water Research* **2003**, 37 (6), 1308-1319.
18. Zhang, L.; Lei, J.; Ma, F.; Ling, P.; Liu, J.; Ju, H., *Chemical Communications* **2015**, 51 (54), 10831-10834.
19. Adarsh, N.; Avirah, R. R.; Ramaiah, D., *Organic Letters* **2010**, 12 (24), 5720-5723.
20. Crosby, G. A.; Demas, J. N., *The Journal of Physical Chemistry* **1971**, 75 (8), 991-1024.
21. Rockley, M. G.; Waugh, K. M., *Chemical Physics Letters* **1978**, 54 (3), 597-599.
22. Aebisher, D.; Zamadar, M.; Mahendran, A.; Ghosh, G.; McEntee, C.; Greer, A., *Photochemistry and Photobiology* **2010**, 86 (4), 890-894.

23. C. Rota, C. F. Chignell, R. P. Mason, *Free Radical Biology and Medicine* **1999**, *27*, 873-881.
24. Felgenträger, Ariane et al. *BioMed research international* **2013**, vol. 2013, 482167.
25. aQ.-Y. Chen, M.-Y. Kong, P.-D. Wang, S.-C. Meng, X.-L. Xu, *RSC Advances* **2014**, *4*, 50693-50698; bS.-y. Takizawa, R. Aboshi, S. Murata, *Photochemical & Photobiological Sciences* **2011**, *10*, 895-903; cW.-T. Wu, L.-Y. Zhan, W.-Y. Fan, X.-Y. Wu, Q.-W. Pan, L. Huang, Z.-T. Li, J.-T. Zheng, Y.-F. Wang, M.-B. Wu, *Macromolecular Chemistry and Physics* **2014**, *215*, 280-285; dJ. R. Herschmann, A. Ali, M. Harris, M. McClinton, M. Zamadar, *Photochemistry and Photobiology* **2019**, *95*, 823-832.
26. T. Gensch, C. Viappiani, S. E. Braslavsky, *Journal of the American Chemical Society* **1999**, *121*, 10573-10582.
27. F. Wilkinson, W. P. Helman, A. B. Ross, *Journal of Physical and Chemical Reference Data* **1993**, *22*, 113-262.
28. N. N. Kruk, B. M. Dzhagarov, V. A. Galievsky, V. S. Chirvony, P.-Y. Turpin, *Journal of Photochemistry and Photobiology B: Biology* **1998**, *42*, 181-190.
29. T. Ahmad, Y. J. Suzuki, *Antioxidants (Basel)* **2019**, *8*, 91.
30. M. G. Alemseghed, T. P. A. Ruberu, J. Vela, *Chemistry of Materials* **2011**, *23*, 3571-3579.
31. aW. Zhang, A. Liu, Y. Li, X. Zhao, S. Lv, W. Zhu, Y. Jin, *Canadian Journal of Physiology and Pharmacology* **2012**, *90*, 1553-1558; bT. Liu, Y. Li, N. Li, *BIO Web*

- Conf.* **2017**, 8, 01013; cF. Fang, Y. Qin, L. Qi, Q. Fang, L. Zhao, S. Chen, Q. Li, D. Zhang, L. Wang, *Iranian Journal of Basic Medical Sciences* **2015**, 18, 544-548.
32. S. V. Torti, F. M. Torti, *Nature Reviews Cancer* **2013**, 13, 342.
33. Y. Ito, *Bioconjugate Chemistry* **1993**, 4, 127-133.
34. K. A. Hislop, J. R. Bolton, *Environmental Science & Technology* **1999**, 33, 3119-3126.
35. aC. Bizet, P. Morlière, D. Brault, O. Delgado, M. Bazin, R. Santus, *Photochemistry and Photobiology* **1981**, 34, 315-321; bM. Faraggi, A. Carmichael, P. Riesz, *International Journal of Radiation Biology and Related Studies in Physics, Chemistry and Medicine* **1984**, 46, 703-713; cT. Akira, S. Mitsuo, *Chemistry Letters* **1989**, 18, 153-156.
36. R. Sreekanth, K. P. Prasanthkumar, M. M. Sunil Paul, U. K. Aravind, C. T. Aravindakumar, *The Journal of Physical Chemistry A* **2013**, 117, 11261-11270.
37. aJ. De Laat, G. Truong Le, B. Legube, *Chemosphere* **2004**, 55, 715-723; bJ. De Laat, T. G. Le, *Environmental Science & Technology* **2005**, 39, 1811-1818; cP. J. Novak, S. J. Christ, G. F. Parkin, *Water Research* **1997**, 31, 3107-3115.
38. A. M. Kabel, *World Journal of Nutrition and Health* **2014**, 2, 35-38.
39. aG. D. Mao, P. D. Thomas, G. D. Lopaschuk, M. J. Poznansky, *Journal of Biological Chemistry* **1993**, 268, 416-420; bK. Isuzugawa, M. Inoue, Y. Ogihara, *Biological and Pharmaceutical Bulletin* **2001**, 24, 1022-1026.

40. Lisanti, M. P.; Martinez-Outschoorn, U. E.; Lin, Z.; Pavlides, S.; Whitaker-Menezes, D.; Pestell, R. G.; Howell, A.; Sotgia, F. *Cell cycle (Georgetown, Tex.)*, **2011**, *10*(15), 2440–2449.
41. aL. Zhang, J. Lei, F. Ma, P. Ling, J. Liu, H. Ju, *Chemical Communications* **2015**, *51*, 10831-10834; bM. G. Rockley, K. M. Waugh, *Chemical Physics Letters* **1978**, *54*, 597-599.
42. L. Zhang, J. Lei, F. Ma, P. Ling, J. Liu, H. Ju, *Chemical Communications* **2015**, *51*, 10831-10834.
43. J. Wang, Y. Cheng, R. Wu, D. Jiang, B. Bai, D. Tan, T. Yan, X. Sun, Q. Zhang, Z. Wu, *International Journal of Molecular Sciences* **2016**, *17*, 965.

VITA

After graduating from William P. Clements High School in 2015, Aqeeb Ali moved from Richmond, Texas to attend Stephen F. Austin State University at Nacogdoches, Texas. He graduated with a Bachelor of Science in Chemistry in May 2019 and furthered his education by enrolling in Graduate School at Stephen F. Austin State University. He graduated with a degree of Master of Natural Science in May 2021.

Permanent Address: 1826 Andrew Oaks Ct.
Richmond, TX 77469

The American Chemical Society (ACS) Style Guide

This thesis was typed by Aqeeb Ali